HHS Public Access

Author manuscript

Neurobiol Dis. Author manuscript; available in PMC 2024 February 16.

Published in final edited form as:

Neurobiol Dis. 2024 February ; 191: 106411. doi:10.1016/j.nbd.2024.106411.

Neuroinflammatory gene expression profiles of reactive glia in the substantia nigra suggest a multidimensional immune response to alpha synuclein inclusions

Anna C. Stoll[a,b], **Christopher J. Kemp**[a], **Joseph R. Patterson**[a], **Jacob W. Howe**[a], **Kathy Steece-Collier**[a], **Kelvin C. Luk**[c], **Caryl E. Sortwell**[a,1], **Matthew J. Benskey**[a,*,1]

[a]Department of Translational Neuroscience, Michigan State University, Grand Rapids, MI, USA

[b]Department of Pharmacology and Toxicology, Michigan State University, East Lansing, MI, USA

[c]Center for Neurodegenerative Disease Research, Department of Pathology and Laboratory Medicine, University of Pennsylvania Perelman School of Medicine, Philadelphia, PA, USA

Abstract

Parkinson's disease (PD) pathology is characterized by alpha-synuclein (α-syn) aggregates, degeneration of dopamine neurons in the substantia nigra pars compacta (SNpc), and neuroinflammation. The presence of reactive glia correlates with deposition of pathological α-syn in early-stage PD. Thus, understanding the neuroinflammatory response of microglia and astrocytes to synucleinopathy may identify therapeutic targets. Here we characterized the neuroinflammatory gene expression profile of reactive microglia and astrocytes in the SNpc during early synucleinopathy in the rat α-syn pre-formed fibril (PFF) model. Rats received intrastriatal injection of α-syn PFFs and expression of immune genes was quantified with droplet digital PCR (ddPCR), after which fluorescent in situ hybridization (FISH) was used to localize gene expression to microglia or astrocytes in the SNpc. Genes previously associated with reactive microglia (*Cd74*, *C1qa*, *Stat1, Axl, Casp1, Il18, Lyz2*) and reactive astrocytes (*C3, Gbp2, Serping1*) were significantly upregulated in the SN of PFF injected rats. Localization of gene expression to SNpc microglia near α-syn aggregates identified a unique α-syn aggregate microglial gene expression profile characterized by upregulation of *Cd74, Cxcl10, Rt-1a2, Grn, Csf1r, Tyrobp, C3, C1qa, Serping1* and *Fcer1g*. Importantly, significant microglial upregulation of *Cd74* and *C3* were only observed following injection of α-syn PFFs, not α-syn monomer, confirming specificity to α-syn aggregation. *Serping1* expression also localized to astrocytes in the SNpc. Interestingly,

*Corresponding author at: Department of Translational Neuroscience, Michigan State University, Grand Rapids, MI 49503, USA. benskeym@msu.edu (M.J. Benskey).

[1]These authors have contributed equally to this work.

Authors contributions

Conception of the study: ACS, CES, MJB; Design of the study: ACS, CES, MJB; Acquisition of study results: ACS, CES, MJB, CJK, JRP, KSC, KCL; Interpretation of study results: ACS, CJK, MJB; Drafting and revisions of manuscript: ACS, CES, MJB.

Crdit author statement

CES and MJB conceived studies and designed experiments. ACS, CJK, JRP, JWH, CES and MJB performed surgery. KCL supplied recombinant alpha synuclein. ACS, CJK, KSC and MJB acquired data. MJB, ACS and CES performed data analysis. MJB, ACS and CES drafted and edited the manuscript. CES and MJB acquired financial support for the project.

Appendix A. Supplementary data

Supplementary data to this article can be found online at https://doi.org/10.1016/j.nbd.2024.106411.

C3 expression in the SNpc localized to microglia at 2- and 4-months post-PFF, but to astrocytes at 6-months post-PFF. We also observed expression of *Rt1-a2* and *Cxcl10* in SNpc dopamine neurons. Cumulatively our results identify a dynamic, yet reproducible gene expression profile of reactive microglia and astrocytes associated with early synucleinopathy in the rat SNpc.

Keywords

Glia; Microglia; Astrocyte; Alpha-synuclein; Neuroinflammation; Parkinson's disease; Synucleinopathy

1. Introduction

Parkinson's Disease (PD) pathology is characterized by intra-neuronal aggregates (Lewy bodies) enriched in the protein alpha-synuclein (α-syn), and progressive loss of nigrostriatal dopamine (DA) neurons. While the etiology of PD is unclear, evidence suggests neuroinflammation, mediated both by the innate and adaptive immune systems, contributes to pathogenesis (Tansey et al., 2022a, 2022b; Tansey and Romero-Ramos, 2019). For instance, pro-inflammatory cytokines are increased in the substantia nigra (SN), cerebrospinal fluid (CSF), and blood of PD patients, where levels of certain cytokines directly correlate with the degree of clinical symptomology and pathology (Ahmadi Rastegar et al., 2019; Blum-Degena et al., 1995; Brodacki et al., 2008; Chen et al., 2018; Karpenko et al., 2018; Mogi et al., 1996, 1994b, 1994a; Müller et al., 1998; Qin et al., 2016; Reale et al., 2009; Williams-Gray et al., 2016). Epidemiological data also support a role for neuroinflammation in the pathogenesis of PD. For example, chronic use of ibuprofen (Chen et al., 2005, n.d.; Gao et al., 2011; Samii et al., 2009) and anti-tumor necrosis factor (TNF) therapy (Park et al., 2019; Peter et al., 2018) are associated with decreased risk of PD, while SNPs in the HLA-DR gene (encoding MHC-II) are associated with increasedrisk of developing PD (Hamza et al., 2010). Infiltration of T-cells in the brains of PD patient and deposition of IgG on neuromelanin containing neurons in the PD SNpc support a role for an adaptive immune response (Cebrián et al., 2014; Loeffler et al., 2006; Orr et al., 2005; Yamada et al., 1992). Of particular interest is the role glia play in PD pathology, as gliosis closely tracks with PD progression. For instance, both postmortem and in-vivo PET imaging studies reveal increased numbers of activated microglia in PD affected brain regions (Croisier et al., 2005; Dijkstra et al., 2015; Gerhard et al., 2006; Lavisse et al., 2021; Liu et al., 2022; McGeer et al., 1988; Ouchi et al., 2005; Terada et al., 2016; Zhang and Gao, 2022). In the brain, reactive microglia are the major source of cytokine and chemokine production, suggesting an early activation of microglia may mediate neuroinflammation through the release of proinflammatory molecules. Indeed, in vivo imaging using ligands of translocator protein 18kd (TSPO) as a marker of neuroinflammation demonstrate significantly elevated TSPO signal in disease affected brain regions of early stage, untreated PD patients (Ouchi et al., 2005; Yacoubian et al., 2023; Zhang and Gao, 2022). Further, both CSF and blood cytokines/chemokines are increased in early-stage PD patients (Zimmermann and Brockmann, 2022), some of which directly correlate with the level of TSPO signal in the brain(Liu et al., 2022; Yacoubian et al., 2023). Finally, increased levels of α-syn reactive T-cells are detected in the blood of

prodromal PD patients, which then decline following the clinical onset of motor symptoms (Lindestam Arlehamn et al., 2020). These data suggest an initial immunogenic stimulus triggers neuroinflammation in early-stage PD, prior to overt neurodegeneration, after which reactive glia and peripheral leukocytes may actively contribute to neurotoxicity. As such, understanding the early events in PD-associated neuroinflammation could yield insights into the pathogenic mechanisms driving disease progression.

The aggregation of α-syn likely represents one immunogenic stimulus driving the immune response in PD. In the PD brain, α-syn aggregation correlates both spatially and temporally with the presence of activated microglia (Croisier et al., 2005; Imamura et al., 2003), Lewy bodies are coated with immunoglobulins and complement proteins (Loeffler et al., 2006; Orr et al., 2005), and T-cells from PD patients are activated by peptides derived from α-syn (Cebrián et al., 2014; Lindestam Arlehamn et al., 2020; Sulzer et al., 2017). Further, similar neuroinflammatory changes are observed in other synucleinopathies (Compta et al., 2019; Gate et al., 2021; Kübler et al., 2019; Streit and Xue, 2016; Surendranathan et al., 2018; Williams et al., 2020), suggesting neuroinflammation is a common response to α-syn aggregation. Supporting this, neuroinflammation is a prominent feature of the rat α-syn preformed fibril (PFF) model of synucleinopathy (Duffy et al., 2018; Miller et al., 2021; Stoll et al., 2023; Stoll and Sortwell, 2022). We have performed a detailed characterization of this model and have identified two distinct pathological phases in the substantia nigra pars compacta (SNpc) following intrastriatal injection of α-syn PFFs (Duffy et al., 2018; Patterson et al., 2019a; Stoll and Sortwell, 2022). The first phase, or “aggregation phase”, occurs 1–2 months post-injection and is characterized by peak accumulation of “Lewy body-like” protein aggregates composed of endogenous α-syn phosphorylated at serine 129 (pSyn) (Patterson et al., 2019a; Paumier et al., 2015). The second phase, or “degenerative phase”, occurs 2–6 months post-injection and is characterized by protracted degeneration of nigrostriatal dopamine (DA) neurons (Patterson et al., 2019a; Paumier et al., 2015). Importantly, the aggregation phase in the α-syn PFF model is associated with pronounced gliosis. In the SNpc 2-months post-PFF, microglial numbers are increased, microglia increase expression of MHC-II and display a reactive morphology (Duffy et al., 2018). In parallel, we observe increased levels of glial fibrillary acidic protein (GFAP) and increased length and branching of astrocyte processes in the SNpc (Miller et al., 2021), indicating activation of astrocytes. Importantly, these indices of gliosis occur in the immediate vicinity of α-syn inclusions, significantly correlate with numbers of pSyn+ neurons in the SNpc and appear months prior to overt neurodegeneration. Taken together, these data suggest neuroinflammation, mediated at least in part by reactive microglia and astrocytes, may contribute to neurotoxicity in response to synucleinopathy.

Although previous reports have demonstrated changes commonly associated with reactive astrocytes (e.g. increased GFAP expression and branching) and reactive microglia (e.g. MHC-II expression and changes in morphology) in response to α-syn aggregation, these changes alone do not adequately describe the complex phenotype of reactive glia associated with early synucleinopathy in the SNpc. Reactive gliosis refers not only to the morphologic, but also molecular and functional changes in glia (astrocytes, microglia and to a lesser extent NG2+ oligodendrocyte progenitors) in response to CNS insult (Escartin et al., 2021; Paolicelli et al., 2022). Recent advances in single cell profiling of glial cells

reveal tremendous heterogeneity in both reactive astrocytes and microglia that is context dependent. For example, the specific type and relative abundance of different reactive glial populations that emerge following CNS insult depends on a constellation of interacting factors including, but not limited to, the specific type of insult, the severity and time course of the insult, and the subregion of the CNS in which the glia reside (Burda and Sofroniew, 2014; Escartin et al., 2021; Hasel et al., 2023). Further, reactive glia do not fall into binary classifications such as M1/M2-microglia or A1/A2-astrocytes. Rather, reactive gliosis presents on a spectrum, where the emergent function of individual reactive glia is defined by the balance between the loss of normal homeostatic function versus the gain of new protective/detrimental functions (Escartin et al., 2021; Paolicelli et al., 2022). The net impact of reactive gliosis on disease pathogenesis is determined by the relative abundance of different reactive glial populations (both within- and between different glial lineages, i.e. astrocytes and microglia) and the balance of gained versus lost glial functions. Accordingly, a detailed understanding of the insult specific reactive glial phenotype present within an affected brain region should allow for identification of potential points of therapeutic intervention. To this end, the goal of the current study is to provide a more comprehensive characterization of the phenotype of reactive astrocytes and microglia in the SNpc during the early phases of synucleinopathy in the rat α-syn PFF model.

Reactive glia rapidly alter gene expression to tailor their response to specific insults, and the unique profile of differentially expressed genes can be used to phenotype distinct populations of reactive glia (Escartin et al., 2021; Hasel et al., 2023; Paolicelli et al., 2022). Therefore, in the current study we used changes in gene expression to characterize the phenotype of reactive glia in the SN/SNpc during the early phases of synucleinopathy in α-syn PFF injected rats. To characterize the synucleinopathy associated reactive glia gene expression profile we utilized two complementary approaches. The first approach was to probe for changes in immune genes that are upregulated in PD, Alzheimer's disease (AD) or preclinical models of neurodegenerative disease (Barnum and Tansey, 2010; Bettcher et al., 2021; Boche and Gordon, 2022; Deczkowska et al., 2018; Dubbelaar et al., 2018; Heidari et al., 2022a; Keren-Shaul et al., 2017; Liddelow et al., 2020, 2017a, 2017b; Mathys et al., 2017a; Morgan and Mielke, 2021; Sanchez-Guajardo et al., 2013; Smajić et al., 2022a; Tansey and Romero-Ramos, 2019; Zamanian et al., 2012). For this experiment we used droplet digital PCR (ddPCR) to quantify changes in the expression of select immune genes in the SN during the aggregation phase of the rat α-syn PFF model (2-months post PFF; peak of α-syn inclusion formation and reactive microgliosis/astrogliosis).

The second approach towards developing a synucleinopathy associated reactive glia gene expression profile was to localize the cellular source of upregulated immune genes in the rat SNpc following PFF-induced synucleinopathy. Recently our laboratory used an unbiased, refined bulk RNA-Seq approach to analyze transcript levels in the SNpc during the aggregation phase of the α-syn PFF model ((Patterson et al., 2024) This dataset identified multiple upregulated transcripts associated with innate and adaptive immune pathways (i.e antigen presentation, natural killer cell mediated cytotoxicity, complement pathway, T-cell activation, inflammasome activation). In the present study we sought to expand and validate these findings and identify astrocytes, microglia, or MHC-II+ microglia as cellular sources of select upregulated transcripts previously identified using RNA-Seq. For this experiment

we used in-situ hybridization to localize the cellular source of transcripts in the SNpc during the aggregation phase of the α-syn PFF model. Using these two complementary approaches we have generated a gene expression signature of reactive microglia in the rat SNpc during the early stages of synucleinopathy (prior to overt neurodegeneration).

Specifically, this unique approach identified gene expression signatures that suggest: 1) a suite of immune genes that are upregulated by both astrocytes and microglia in the SNpc during peak α-syn aggregation; and 2) a specific α-syn aggregate microglial gene expression profile observed in reactive microglia in the immediate vicinity of α-syn inclusions. Taken together we show early synucleinopathy increases gene expression associated with a diverse array of immune functions, including complement, inflammasome, T-cell activation, phagocytosis, and interferon gamma signaling. A comprehensive understanding of the multidimensional response of reactive glia to synucleinopathy may identify novel therapeutic targets and facilitate development of disease-modifying strategies for PD.

2. Methods

2.1. Experimental overview

2.1.1. Experiment 1: ddPCR based quantification of synucleinopathy associated changes in gene expression—For this experiment we performed a literature review to identify immune genes that are upregulated in PD, AD or preclinical models of neurodegenerative disease (Barnum and Tansey, 2010; Bettcher et al., 2021; Boche and Gordon, 2022; Deczkowska et al., 2018; Dubbelaar et al., 2018; Heidari et al., 2022a; Keren-Shaul et al., 2017; Liddelow et al., 2020, 2017a, 2017b; Mathys et al., 2017a; Morgan and Mielke, 2021; Sanchez-Guajardo et al., 2013; Smajić et al., 2022a; Tansey and Romero-Ramos, 2019; Zamanian et al., 2012). Following identification of upregulated immune genes, male and female rats (n = 10–20/group) received unilateral intrastriatal injections of either α-syn PFFs or phosphate buffered saline (PBS) and were euthanized 2-months post-injection (peak α-syn aggregation and gliosis in the SNpc). RNA was extracted from SN tissue and ddPCR was used to quantify expression of the selected immune genes. Supplemental Fig. 1 A illustrates the experimental design.

2.1.2. Experiment 2: histologic investigation into the cellular identity of innate immune transcripts associated with synucleinopathy—We investigated whether microglia, MHC-II immunoreactive microglia, or astrocytes were the cellular source of select upregulated immune transcripts previously identified using RNA-Seq in association with early synucleinopathy in the SNpc of PFF injected male rats. In a previous study (Patterson et al., 2024), an unbiased refined bulk RNAseq approach identified 176 upregulated transcripts associated with immune-related pathways and with known expression in microglia (Saunders et al., 2018) in both male and female rats. From the list of differentially expressed genes an a priori cutoff value of genes with >15 transcripts per million (TPM) in PFF injected male rats were used to select genes (as this level of expression is necessary to detect RNA via in situ hybridization). Rats received unilateral intrastriatal injections of either α-syn PFFs or (n = 5), α-syn monomer (n = 5) or phosphate buffered saline (n = 5) and were euthanized 2 months post injection (peak SNpc α-syn

aggregation and gliosis). Fluorescence in situ hybridization (FISH, RNAscope™) combined with immunofluorescence (IF) was used to determine the cellular source of selected transcripts in the SNpc. Supplemental Fig. 1B illustrates the experimental design.

2.2. Animals

Three-month old, male and female Fischer 344 rats (Charles River; FISH n = 10; ddPCR n = 10–20/group) were housed, 2–3 per cage, at the Grand Rapids Research Center which is fully approved through the Association for Assessment and Accreditation of Laboratory Animal Care (AAALAC). Rats were housed in a room with a 12-h light/dark cycle and provided food and water ad libitum. All procedures were done in accordance with the guidelines set by the Institutional Animal Care and Use Committee (IACUC) of Michigan State University.

2.3. α-syn PFF preparation and fibril size verification

Preformed fibrils were generated from wild-type, full length, recombinant mouse α-syn monomers as previously described (Luk et al., 2012; Patterson et al., 2019b; Polinski et al., 2018; Volpicelli-Daley et al., 2014, 2011). Quality control was completed on full length fibrils to ensure fibril formation (transmission electron microscopy), amyloid structure (thioflavin T assay), pelletability as compared to monomers (sedimentation assay), and low endotoxin contamination (*Limulus* amebocyte lysate assay; <0.5 endotoxin units/mg of total protein). All quality control (except transmission electron microscopy of sonicated PFFs) was conducted by the Luk lab at the University of Pennsylvania. On surgery day, PFFs were thawed to room temperature and diluted to 4μg/μl in sterile Dulbecco's phosphate buffered saline (dPBS) and sonicated with an ultrasonic homogenizer (300 VT; Biologics, Inc.) for 60 × 1 s pulses with pulser at 20% and power output at 30%. An aliquot of sonicated PFFs was analyzed using transmission electron microscopy (TEM; Supplemental Fig. 1C). For TEM, aliquoted PFFs were prepared on Formvar/carbon-coated copper grids (EMSDIASUM, FCF300-Cu). Grids were washed twice with 10 μl drops of ddH2O, then incubated in 10 μl of sonicated PFFs diluted 1:50 in sterile PBS for 1 min, followed by a 1-min incubation in 10 μl of aqueous 2% uranyl acetate. Grids were allowed to dry fully before being imaged with a JEOL JEM-1400+ transmission electron microscope. Post-surgery, fibril lengths were measured using ImageJ 1.53 K (Wayne Rasband and contributors, National Institutes of Health, USA) to ensure samples contained PFFs of appropriate length necessary for efficient seeding of endogenous α-syn in neurons (fibril length < 50 nm is required for successful seeding of endogenous α-syn inclusions (Tarutani et al., 2016)).The mean length of sonicated PFFs for the ddPCR surgical cohort (experiment 1) was 39.97 ± 0.76 nm and mean length of PFFs for the histological surgical cohort (experiment 2) was 37.82 ± 0.67 nm (Supplemental Fig. 1C–D).

2.4. Stereotaxic injections

Unilateral intrastriatal injections of α-syn PFFs, α-syn monomer or dPBS vehicle control were conducted as previously described (Patterson et al., 2019a). Rats were anesthetized with isoflurane (5% induction and 1.5% maintenance) and received unilateral intrastriatal injections to the left hemisphere (2 injections of 2 μl each). Site 1: AP +1.6, ML +2.0, DV −4.0; Site 2: AP +0.1, ML +4.2, DV −5.0. All AP and ML coordinates relative to Bregma,

DV coordinates relative to dura. α-syn PFFs or α-syn monomer (4 μg/μl; 16 μg total) or an equal volume of dPBS were injected at a rate of 0.5 μl/min with a pulled glass capillary tube attached to a 10 μl Hamilton syringe. After each injection the needle was left in place for 1 min, retracted 0.5 mm and left for 2 min to avoid reflux, and then fully retracted. All animals received analgesic (1.2 mg/kg of sustained release buprenorphine) after surgery and monitored until euthanasia.

2.5. Euthanasia and tissue preparation

Animals were euthanized at 2, 4 or 6 months post-injection using a lethal 30 mg/kg i.p. injection of pentobarbital (Euthanasia-III Solution, MED-PHARMEX Incorporated) and perfused intracardially with heparinized (10,000 units per liter) 0.9% saline.

2.5.1. Experiment 1: ddPCR based quantification of synucleinopathy associated changes in gene expression—

Brains were removed, and flash frozen in 2-methylbutane on dry ice for 10–20 s and subsequently stored at −80°C. Frozen brains were mounted in OTC and sectioned on a cryostat to the level of the rostral SN. The ipsilateral SN, including the SNpc, was microdissected (1 mm (tall) × 2 mm (wide) oval punch) at −15°C. Tissue was collected in DNase/RNase free microcentrifuge tubes containing 100 μl TRIzol reagent (Invitrogen 26,696,026), homogenized with a disposable pestle, volume of TRIzol was brought to 1 mL, triturated, and samples were frozen on dry ice and stored at −80°C.

2.5.2. Experiment 2: histologic investigation into the cellular identity of innate immune transcripts associated with synucleinopathy—

Brains were removed and post-fixed in 4% paraformaldehyde for one week and then transferred to 30% sucrose in 0.1 M phosphate buffer for cryopreservation. Brains were frozen with dry ice and sectioned coronally at 40 μm (6 series of sections) on a sliding microtome and stored in cryoprotectant (30% sucrose, 30% ethylene glycol, in 0.1 M Phosphate Buffer, pH 7.3) at −20 °C.

2.6. RNA isolation

RNA isolation was conducted as described previously (Patterson et al., 2022). Tissue punches in TRIzol were thawed on ice and briefly centrifuged. Phasemaker microcentrifuge tubes (Invitrogen, A33248) were prepared according to manufacturer specifications. Samples were transferred to Phasemaker tubes and incubated at room temperature (RT) for 5 mins, followed by an addition of 200 μl of chloroform and incubated at RT for 10 mins. The tubes were centrifuged for 5 mins at 16,000 ×g at 4°C, the aqueous phase was transferred to an RNase free tube and an equal volume of 100% ethanol was added and vortexed. A column-based RNA purification kit (Zymo Research, R1016) was used according to the manufacturer's instructions with slight modification. 600 μl of sample was added to the column at a time, and centrifuged for 1 min at 12,000 ×g until the entire sample has been added. All wash and prep buffer steps were performed by adding the buffer to the column followed by centrifugation for 1min at 12,000 ×g. Samples were first washed with 400 μl of RNA wash buffer. The membranes of the RNA purification columns were then incubated with a DNase I cocktail (DNase I from Thermo Scientific FEREN0521; Reaction buffer

with MgCl2 from Thermo Scientific FERB43) and incubated at RT for 15 min to remove any contaminating DNA. Columns were then centrifuged, followed by addition of 400 µl of RNA prep buffer and centrifugation. Columns were washed 2× with RNA wash buffer (700 µl then 400 µl), an extra centrifugation step was done for 2 mins to dry the column. 15 µl of DNase/RNase free water was added to the column and incubated for 1 min then eluted by centrifugation at 10,000 *g* for 1 min. Quality and quantity of RNA was assessed with Agilent 2100 Bioanalyzer using an Agilent RNA 6000 Pico Kit (5067–1513). RNA was diluted to 1ng/µL with DNase/RNase free water, aliquoted and stored at −80°C.

2.7. ddPCR

RNA was thawed on ice and 2–10 ng (based on RNA input optimization experiments for each individual probe) was mixed with iScript Reverse Transcription Supermix for cDNA synthesis (Bio-Rad, 1,708,841). Thermocycler setting for cDNA synthesis: 5mins at 25°C, 20mins at 46°C, 1min at 95°C, hold at 4°C (constant lid temperature of 105°C). cDNA was diluted with 2× cDNA storage buffer (equal parts 10mM Tris HCl pH 7.5, and 0.1mM EDTA pH 8.0) and stored at −20°C. TaqMan Gene Expression Probes (Applied Biosystems #4331182) were used for ddPCR. All respective probes (See Supplemental Table 1 for probe details) were specific to rat transcripts and spanned exon-exon junctions to ensure analysis of mature mRNA. For ddPCR reactions, 11 µl of cDNA was mixed with 11 µl of ddPCR master mix (1× ddPCR supermix for probes no dUTP (BioRad 1,863,024), 1ul of probe of interest conjugated to FAM fluorophore, and 0.5ul of *Rpl13* probe conjugated to VIC fluorophore) were added to PCR tubes, mixed, and briefly centrifuged. 20µL of the cDNA-master mix reaction was added to the sample wells of DG8 droplet generator cartridges (Bio-Rad, 1,864,008). 70µL of droplet generation oil (Bio-Rad, 1,863,005) was added to each oil well in the cartridge. A rubber gasket (Bio-Rad, 1,863,009) was secured over the cartridge, and a QX droplet generator (Bio-Rad, 186–4002) was used to produce cDNA/ddPCR mastermix containing droplets. 40µL of droplets were transferred to a 96-well plate (Bio-Rad, 12,001,925) and sealed with pierceable foil (Bio-Rad, 181–4040) by a plate sealer (Bio-Rad, 181–4000). Plates were transferred to a thermocycler (Bio-Rad, C1000), and the PCR reaction was carried out with the following settings: 10mins at 95°C, 39 cycles (30s at 94°C, 1min at 60°C), 10mins at 98°C, hold at 12°C (constant lid temperature of 105°C). Plates were then transferred to the QX200 droplet reader (Bio-Rad, 1,864,003), and results analyzed with QuantaSoft software. For all samples, the gene of interest was normalized to the reference gene, *Rpl13*.

2.8. Immunohistochemistry and stereological quantification of pSyn ± SNpc neurons

Free floating sections were washed 4 × 5 min in 0.1 M tris buffered saline (TBS) containing 0.5% Triton X-100 (TBS-Tx), quenched in 3% H_2O_2 for 1 h, blocked in 10% normal goat serum (NGS) in TBX-Tx, and incubated overnight in primary antibody in 1% NGS/TBS-Tx at 4 °C on a shaker. Primary antibodies used included: mouse anti-α-syn phosphorylated at serine 129 (pSyn) (1:10,000; Abcam, AB184674; RRID: AB_2819037) and mouse anti-major histocompatibility complex-II (MHC Class II RT1B clone OX-6) (1:2000; BioRad, MCA46G; RRID: AB_322113). Sections were washed in TBS-Tx and then incubated for 2-h at room temperature with biotinylated goat anti-mouse IgG (1:500; Millipore, AP124B; RRID: AB_92458) secondary antibody in 1% NGS/TBS-Tx. Sections were washed 4 ×

5 min in TBS-Tx and incubated in standard avidin-biotin complex detection kit (ABC, Vector Laboratories, PK-6100; RRID: AB_2336819). Visualization for pSyn was done using 0.5 mg/ml diaminobenzidine (Sigma-Aldrich, D5637), and 0.03% H_2O_2 in TBS-Tx. MHC-II was visualized using Vector ImmPACT DAB Peroxidase kit (Vector Laboratories; SK-4105). Sections were mounted, allowed to dry, rehydrated, then dehydrated in ascending ethanol washes and cleared with xylene before cover slipping using Epredia Cytoseal-60 (Thermo-Fisher, 22–050–262). Total enumeration was used for quantification of pSyn immunoreactive (pSyn+) neurons, conducted utilizing Microbrightfield Stereoinvestigator (MBF Bioscience). Sections containing the SNpc (1:6 series) were used. Contours were drawn around the SNpc at 4×, a 20× magnification was then used for identification and counting. Counts represent the raw total number multiplied by six (to account for the section series).

2.9. Immunofluorescence (IF)

Free floating sections were washed 6 × 10 min in 0.1 M tris buffered saline containing 0.5% triton x-100 (TBS-Tx), blocked in 10% normal goat serum (NGS) in TBX-Tx for 1 h, then incubated overnight in primary antibodies diluted in TBS-Tx containing 1% NGS at 4 °C on a shaker. Primary antibodies used were mouse anti-pSyn (1:10000; Abcam, AB184674; RRID: AB_2819037) and rabbit anti-tyrosine hydroxylase (TH) (1:4000; Millipore, AB152; RRID: AB_390204). Following primary antibody incubation, sections were washed 6 × 10 min in TBS-Tx and then incubated for 2-h, in the dark, at RT, with fluorescent conjugated secondary antibodies diluted in TBS-Tx containing 1% NGS. Secondary antibodies used: Alexa Fluor 594 goat anti-mouse IgG2a (1:500, Invitrogen, A21135; RRID: AB_2535774), Alexa Fluor 488 goat anti-rabbit IgG (1:500, Invitrogen, A11034; RRID: AB_2576217). Sections were then washed 6 × 10 min in TBS-Tx, incubated in 4′,6-Diamidino-2-Phenylindole, Dihydrochloride (DAPI) diluted in TBS-Tx (1:10,000, Invitrogen, D1306: RRID: 2629482) for 5 min, and placed back in TBS-Tx for mounting. Sections were mounted on HistoBond+ slides (VWR VistaVision, 16,004–406) slides and cover-slipped with VECTASHIELD Vibrance antifade mounting medium (Vector Laboratories, H-1700) and kept in the dark until imaging. Images were taken using Nikon Eclipse Ni–U microscope with CFI60 infinity optical system (Nikon Instruments Inc.) using the 20× and 40× objectives.

2.10. RNAscope™ HiPlex fluorescent in situ hybridization combined with immunofluorescence

RNAscope™ HiPlex Fluorescent in situ hybridization (FISH) was performed on nigral tissue sections to determine the cellular localization of a subset of upregulated genes previously associated with α-syn inclusions (Patterson et al., 2024). RNAscope probes were designed and produced by ACD Bio. Custom RNAscope probes were ordered to target the approximate region of the respective transcripts as the ddPCR primer/probe sets used to quantify the transcripts. These regions were selected to span exon-exon boundaries to ensure analysis of mature mRNA. The protocol for RNAscope probes was always optimized using both positive- and negative control, brain specific, RNAscope probes to validate RNA quality and ensure the specificity of the resultant FISH signal. Free floating sections were washed 4 × 10 min in TBS-Tx and then quenched in ACD Bio Hydrogen Peroxide

(Advanced Cell Diagnostics, 322,335) for 1 h. Tissue was then washed 4 × 10 min in TBS-Tx, followed by 2 × 10-min washes in TBS-Tx diluted 1:4 in ultra-pure water. Tissue was mounted on HistoBond+ slides (VWR VistaVision, 16,004–406) and placed on a slide warmer at 60 °C overnight. The slides were then incubated in an ACD RNAscope™ Target Retrieval buffer (diluted 1:10 in ultra-pure water; Advanced Cell Diagnostics, 322,001) warmed to 99 °C for 10 min and then quickly washed 2 × 1 min in ultra-pure water. Tissue sections were outlined with a Super PapPen (IHC World; SPM0928) and 3 drops of ACD protease III (Advanced Cell Diagnostics; 322,337) was added and incubated in a Hybez ™II oven at 40.0 °C (Advanced Cell Diagnostics) for 30 min. Slides were then quickly washed 2 × 1 min in ultra-pure water, and diluted ACD probes (1:50; See Supplemental Table 2 for detailed probe information) were added to the tissue and incubated in the Hybez ™II oven for 2-h. 3 × 30-min amplification steps were done with ACD amplification buffers 1, 2, and 3 respectively (RNAscope™HiPlex12 Detection Reagents (488,550,650) v2; Advanced Cell Diagnostics, 324,410) in a Hybez ™II oven. Between each amplification tissue was went through 2 × 1-min washes in RNAscope™Wash Buffer (1:500 Dilution in ultra-pure water; Advanced Cell Diagnostics, 310,091). Following the 3rd amplification incubation, slides were washed 2 × 1 min and incubated for 15 min in the Hybez oven with the appropriate ACD fluorophores for the tails on the probes (RNAscope™ HiPlex12 Detection Reagents (488,550,650) v2; Advanced Cell Diagnostics, 324,410). Slides were washed 2 × 1 min and blocked in 10% NGS in TBX-Tx for 1-h at room temperature. Sections were then incubated with primary antibodies diluted in TBS-Tx containing 1% NGS overnight at RT in a humidified chamber. Primary antibodies used: mouse anti-pSyn (1:100; Abcam, AB184674; RRID: AB_2819037), rabbit anti-ionized calcium binding adaptor molecule 1 (Iba1; 1:100; Wako, 019–09741; RRID: AB_839504), rabbit anti tyrosine hydroxylase (TH; 1:400, Millipore, AB152; RRID: AB_390204). Slides were washed 2 × 1 min in TBS-Tx and incubated in Alexa Fluor Secondary antibodies diluted in TBS-Tx containing 1% NGS for 2 h at RT. Secondary antibodies used were Alexa Fluor 568-goat anti mouse (1:250; Invitrogen A11031; RRID: AB_144696), and Alexa Fluor 488-goat anti rabbit (1:250; Invitrogen, A11034; RRID: AB_2576217). Slides were washed 2 × 1 min in TBS-Tx and a drop of RNAscope™HiPlex DAPI (Advanced cell Diagnostics; 324,420) was added and left for 1 min. Excess DAPI was removed, and slides were cover slipped with ProLong™ Gold antifade reagent (Invitrogen, P36930). Images were taken using Nikon Eclipse Ni–U microscope with CFI60 infinity optical system (Nikon Instruments Inc.) using the 20× and 40× objectives.

2.11. Colocalizing genes of interest to microglia, astrocytes and neurons

The following strategy was used to localize the cellular source of upregulated transcripts in the SNpc of PFF injected rats. Midbrain tissue sections containing the SNpc from PBS, α-syn monomer and α-syn PFF injected rats were examined by a blinded observer using the FISH and IF combination strategy detailed in Supplemental Table 3. Immediately adjacent sections to those used for FISH/IF analysis were first analyzed using pSyn/TH IF to validate presence or absence of nigral inclusion bearing neurons. Expression of all probes was initially examined for colocalization with both Iba1 IF and *Cd74* FISH to determine expression in reactive microglia in the ipsilateral inclusion-bearing SNpc. Probes in which expression was not observed to be exclusively colocalized to microglia (*C3, Serping1,*

Cxcl10, Rt1-a2) were further examined in additional adjacent sections using IF for S100β or TH or FISH for *GFAP*, to determine if astrocytes or dopamine neurons also expressed the genes of interest.

2.12. STRING protein function network

To understand the functional overlap between the identified proteins a STRING network was created utilizing https://string-db.org. The target species (*Rattus norvegicus)* along with the protein names/identifiers was used to create the network using the following settings: Full string network, confidence of network edges, all active interaction sources, with a medium confidence of 0.400.

2.13. Statistical analysis

All statistical analyses of the results were completed using GraphPad Prism software (version 9, GraphPad, La Jolla, CA). Outliers were assessed with the absolute deviation from the median method (Leys et al., 2013) utilizing the very conservative difference of 2.5× median absolute deviation as the exclusion criterion. Statistical significance was set to $\alpha \leq 0.05$. Comparisons were made between α-syn PFF versus PBS injected rats using a Student's *t*-Test for each gene in the ipsilateral SN.

3. Results

3.1. Early synucleinopathy stimulates upregulation of immune associated transcripts in SN glia

To characterize the phenotype of reactive glia in the SN during the early phases of synucleinopathy, we used ddPCR to quantify the expression of select immune genes that are upregulated in PD, AD or preclinical models of neurodegenerative disease, 2-months following intrastriatal injection of PBS control or α-syn PFFs. The specific genes examined, *Cd74, C3, Gbp2, Stat1, Serping1, C1qa, Clcf1, Casp1, Tm4sf1, Axl, Il18, Osmr, Lyz2, Tlr4, P2ry12, Ggta1, Lpl, Emp1*, and *S100a10*, represent multiple pathways that are altered in glia during the inflammatory response to pathology associated with neurodegenerative disease (i.e., phagocytosis, microglial regulation, astrocyte activation, lysosomal function, cell proliferation, complement cascade, cytokine signaling, and B cell activation) (Boche and Gordon, 2022; Chen and Colonna, 2021; Deczkowska et al., 2018; Dubbelaar et al., 2018; Helmfors et al., 2015; Keren-Shaul et al., 2017; Mathys et al., 2017a; Morgan and Mielke, 2021; Sala Frigerio et al., 2019; Sanchez-Guajardo et al., 2013; Smajić et al., 2022a; Srinivasan et al., 2016; Tansey and Romero-Ramos, 2019). Fig. 1 shows significantly increased expression of genes in the ipsilateral SN of α-syn PFF-injected rats compared to PBS controls, including *Cd74* (Antigen presentation, $p < 0.0001$), *C3* (Complement cascade, $p < 0.0001$), *Gbp2* (interferon gamma and cytokine signaling, $p < 0.001$), *Stat1* (JAK/STAT pathway, $p = 0.0022$), *Serping1* (complement cascade, $p = 0.022$), *C1qa* (Complement cascade, $p < 0.0001$), *Clcf1* (JAK/STAT pathway and B cell activation, $p = 0.0015$), *Casp1* (inflammasome, $p = 0.0021$), *Tm4sf1* (cell growth and proliferation, $p < 0.001$), *Axl* (phagocytosis, $p = 0.0009$), *IL18* (interferon gamma production and inflammasome, $p = 0.0120$), *Osmr* (Oncostatin pathway, $p = 0.0438$), and *Lyz2* (lysosomal function, $p = 0.0364$). Further, some genes previously associated with neuroinflammation in PD or AD

(i.e., *P2Ry12*, *Lpl*, Ggta1, and S100a10) were not altered in the SN of PFF-injected rats at the 2-month time point. These data suggest early synucleinopathy activates multiple immune pathways in the SN prior to neurodegeneration.

3.2. Cellular localization of innate immune transcripts upregulated following synucleinopathy

3.2.1. Microglia in the immediate vicinity of α-syn aggregates respond by upregulating MHC-II and Cd74—

Using a ddPCR approach we detected significant increases in many immune genes associated with reactive glia, however the type of glia expressing the genes is unknown. Thus, we next sought to confirm the cellular source of 3 of the most highly upregulated genes, *Cd74, Serping1*, and *C3*. We utilized FISH with probes targeting *Cd74*, *Serping1*, or *C3* combined with either FISH or IF for either the astrocytic marker, *Gfap*, or the pan microglial marker, Iba1, in the SNpc 2-months post PFF-injection. However, we first confirmed successful α-syn aggregate seeding in the SNpc of PFF injected rats with tissue sections adjacent to those used for FISH analysis. Fig. 2A shows pSyn+ inclusions in tyrosine hydroxylase immunoreactive (THir) SNpc neurons ipsilateral to the injected striatum, confirming successful seeding of α-syn aggregates in nigral neurons.

Next, we identified the cellular source of *Cd74*. *Cd74* is a gene involved in MHC-II trafficking and is normally expressed by border associated macrophages (BAMs) (Utz and Greter, 2019; van Hove et al., 2019). *Cd74*+ cells were almost completely restricted to the ipsilateral SNpc and the region of the ventral meninges (left panel of Fig. 2B), and rarely observed in the contralateral SNpc of PFF-injected rats (Fig. 2E) or the ipsilateral SNpc of PBS-injected rats (data not shown). All *Cd74*+ cells in the ipsilateral SNpc colocalize with Iba1 FISH signal (Fig. 2B), as do the *Cd74*+ cells in the ventral meninges (data not shown), indicating that *Cd74* is expressed by microglia in the SNpc and BAMs in the ventral meninges. To determine whether microglial expression of *Cd74* or MHC-II was specific to α-syn aggregate formation we compared *Cd74* and MHC-II expression in the ipsilateral SNpc of α-syn monomer versus α-syn PFF injected rats 2-months post-injection. Stereological quantification of pSyn+ neurons revealed an average of 2979 ± 350 pSyn+ neurons in the SNpc of PFF injected rats, while no pSyn+ neurons were detected in the SNpc PBS or α-syn monomer injected rats (Fig. 2C). Similarly, parenchymal MHC-II and *Cd74* expression was restricted to the ipsilateral SNpc of PFF injected rats (Fig. 2D, E), with almost no MHC-II+ or *Cd74*+ cells in the SNpc of α-syn monomer or PBS injected rats (Fig. 2D, F). These data suggest a subset of microglia in the immediate vicinity of α-syn aggregates respond by upregulating MHC-II and *Cd74*, confirming and extending our previous findings (Duffy et al., 2018; Miller et al., 2021).

3.2.2. Astrocytes in the immediate vicinity of α-syn aggregates respond by upregulating Serping1—

We next sought to determine the cellular source of *Serping1* expression. Fig. 3A shows *Serping1* expression in *Cd74*+ microglia. However, not all *Serping1* signal colocalized to *Cd74*+ microglia, so we next sought to determine if astrocytes also express *Serping1* in the SNpc of PFF injected rats. Indeed, Fig. 3B shows *Serping1*

FISH signal colocalizes to *Gfap* + astrocytes in the ipsilateral SNpc, confirming the expression of *Serping1* in astrocytes as well as microglia.

3.2.3. Early microglial expression of C3 during pSyn accumulation shifts to astrocytes during later nigral degeneration—Finally, we sought to localize the cell source of *C3* expression. Two-months post-PFF treatment, *C3* FISH revealed expression in Iba1+ microglia in the SNpc (Fig. 3C) but not astrocytes (Supplemental Fig. 2B). To determine if the increase in microglial *C3* expression 2-months post-injection is due to α-syn aggregation, we again compared *C3* expression between α-syn PFF and α-syn monomer injected rats. Robust *C3* FISH signal is observed in the ipsilateral SNpc of PFF injected rats (Fig. 3G), while very little *C3* FISH signal was detected in the SNpc of α-syn monomer injected rats (Fig. 3H–I). Further, *C3* FISH signal in the SNpc of α-syn monomer injected rats was variable, ranging from minimal *C3* expression (Fig. 3H) to almost no *C3* expression (Fig. 3I). *C3* expression in the SNpc of α-syn monomer injected rats is likely an artifact of surgery, as we also observe sparse MHC-II+ cells in the ipsilateral SNpc of PBS injected rats 2-months post-surgery, which decline over time (Duffy et al., 2018). Additionally, the magnitude of C3 upregulation is far greater in α-syn PFF injected rats compared to α-syn monomer injected rats (like MHC-II+ cells in the SNpc of PBS versus α-syn PFF injected rats). Taken together, these data suggest that early accumulation of pSyn+ inclusions in the SNpc stimulates microglia to upregulate expression of *C3*.

C3 is a central component of the complement system and is reported as one of the most consistently and highly upregulated genes expressed by reactive astrocytes (Liddelow et al., 2017b). Thus, we sought to determine if *C3* expression remains restricted to microglia throughout the degenerative time course following initiation of synucleinopathy induced by α-syn PFFs. To this end we performed FISH for *C3* combined with either Iba1 IF or *Gfap* FISH at 4-months post injection (just prior to nigrostriatal degeneration) and 6-months post injection (degenerative phase: ~50–60% loss of nigral neurons). At 4-months post-injection, *C3* FISH signal remains localized to Iba1+ microglia, not *Gfap* + astrocytes (Fig. 3D). However, by 6-months post-injection the majority of *C3* FISH signal no longer colocalizes with Iba1+ microglia (Fig. 3E), but now colocalizes to *Gfap* + astrocytes (Fig. 3F). At this later time point the appearance of the *C3* FISH signal also changed. At the 2–4-month time point, *C3* FISH signal in microglia appears as diffuse puncta (Fig. 3C–E). In contrast, the *C3* FISH signal in *Gfap* + astrocytes at the 6-month time point changes to a dense and highly concentrated morphology (Fig. 3F). These results indicate SNpc astrocytes upregulate *Serping1* in response to synucleinopathy. Further, SNpc microglia upregulate *C3* expression prior to the degenerative phase of synucleinopathy, but at some time between 4- and 6-months, there is a cell type switching, after which astrocytes are the primary cellular source of *C3* in the synucleinopathy affected SNpc.

3.3. Cd74+ microglia in the SNpc upregulate innate immune response transcripts in association with pSyn accumulation

We next sought to determine the cellular source of select upregulated innate immune transcripts previously identified by RNA-Seq analysis of the SNpc in PFF-injected rats (Patterson et al., 2024). To this end we first performed FISH for *Cxcl10, Rt1-a2, Grn,*

Tyrobp, Fger1g, Csf1r, C3 and *C1qa* combined with Iba1 IF (Fig. 4). In the ipsilateral SNpc of PFF injected rats, mRNA for *Cxcl10, Rt1-a2, Grn, Tyrobp, Fger1g, Csf1r, C3* and *C1qa* all localize to Iba1+ microglia (Fig. 4A *Cxcl10*; Fig. 4B *Rt1-a2*; Fig. 4C *Grn*; Fig. 4D *Tyrobp*; Fig. 4E *Fcer1g*; Fig. 4F *Csf1r*; Fig. 4G *C3*; Fig. 4H *C1qa*). These data indicate microglia in the pSyn aggregate bearing SNpc upregulate genes associated with several different immune pathways.

In previous studies, pSyn inclusion load in the SNpc significantly correlates to the number of MHC-II+ microglia in the SNpc (Duffy et al., 2018). *Cd74* mediates assembly and trafficking of MHC-II (Chen and Colonna, 2021; Schröder, 2016) and can be used as a surrogate genetic marker of MHC-II(Jensen et al., 1999). Thus, to determine whether the microglial subpopulation expressing innate immune genes (Fig. 4) is the same MHC-II+ microglial subpopulation correlated to pSyn inclusion load in previous studies, we attempted to colocalize the expression of *Cxcl10, Rt1-a2, Grn, Tyrobp, Fger1g, Csf1r, C3* and *C1qa* to *Cd74*+ microglia. All selected genes colocalize to *Cd74*+ microglia in the ipsilateral SNpc 2 months post-PFF injection (Fig. 4A *Cxcl10*; Fig. 4B *Rt1-a2*; Fig. 4C *Grn*; Fig. 4D *Tyrobp*; Fig. 4E *Fcer1g*; Fig. 4F *Csf1r*; Fig. 4G *C3*; Fig. 4H *C1qa*). These data, combined with earlier findings (Duffy et al., 2018), suggest a subset of *Cd74*+/MHC-II+ microglia in the SNpc upregulate a unique suite of innate immune genes in response to the deposition of pSyn inclusions.

3.3.1. Nigral dopamine neurons in the SNpc express Rt1-a2 and Cxcl10—*Rt1-a2* is upregulated in the ipsilateral SNpc of PFF injected rats (Patterson et al., 2024) where it localizes to Iba1+/*Cd74*+ microglia (Fig. 4A–B). However, we also observe additional *Rt1-a2*+ cells that are Iba1−/ *Cd74*− (arrows in Fig. 5A). *Rt1-a2* encodes a portion of the MHC-I complex and midbrain catecholaminergic neurons express MHC-1 in the PD brain (Cebrián et al., 2014). This suggests other cells in the SNpc also express *Rt1-a2* in response to synucleinopathy, presumably neurons and/or astrocytes (Benskey et al., 2018; Cebrián et al., 2014). To determine if SNpc DA neurons express *Rt1-a2* in response to synucleinopathy, we combined FISH for *Rt1-a2* with IF for TH in the ipsilateral SNpc of PFF injected rats. Indeed, *Rt1-a2* colocalizes to TH+ nigral neurons in the ipsilateral SNpc (Fig. 5B). Surprisingly, TH+ neurons in the contralateral SNpc also expressed *Rt1-a2* (Fig. 5C). Since *Rt1-a2* is also observed in the contralateral hemisphere, which is not affected by α-syn pathology at this early time point, these data suggest dopaminergic neurons in the SNpc express *Rt1-a2* under physiological conditions.

Similar to *Rt1-a2*, *Cxcl10* is upregulated in the SNpc of PFF injected rats (Patterson et al., 2024) where it localizes to IBA1/*Cd74*+ microglia (Fig. 4A). However, we again observe *Cxcl10* FISH signal that does not colocalize with IBA1 or *Cd74* (Fig. 4A). The *Cxcl10* FISH signal that does not colocalize with Iba1/*Cd74* is similar in size and morphology to a nigral neuron soma, suggesting nigral neurons may also express *Cxcl10*. Indeed, *Cxcl10* FISH signal colocalizes with TH IF (arrows in Fig. 5D) but not *Gfap* FISH (Supplemental Fig. 2C), indicating that TH+ neurons in the SNpc of PFF injected rats express *Cxcl10*. Finally, some of the *Cxcl10* FISH signal that resembled the size and morphology of a nigral neuron soma did not colocalize with TH, likely representing a nigral neuron that has lost

its TH phenotype following synucleinopathy (arrowhead in Fig. 5D; (Patterson et al., 2019a; Paumier et al., 2015)).

3.4. Synucleinopathy stimulates a heterogenous but interconnected immune response

To better understand the functional connectivity of the protein products corresponding to the upregulated genes identified in the above experiments we performed a STRING analysis (Supplemental Fig. 3). STRING analyses reveal a highly interconnected network of functions performed by the inflammatory gene products altered during the early phases of synucleinopathy in the SNpc. In this network, virtually every protein for which we identified increased gene expression shows some form of functional connection to the other protein products in the network, highlighting the tremendous functional connectivity between the genes altered and the cell types which expressed the genes.

4. Discussion

The goal of the current study was to identify a reproducible neuroinflammatory gene expression signature associated with reactive glia in the SNpc during the early phases of synucleinopathy (i.e. prior to nigral neuron degeneration). To this end we have identified: 1) a suite of immune genes that are upregulated by astrocytes and microglia in the SNpc during peak α-syn aggregation; and 2) a specific suite of genes that characterize reactive microglia in the immediate vicinity of α-syn inclusions in the rat SNpc. A summary of upregulated genes and their cellular source in the SNpc during peak α-syn aggregation is depicted in Fig. 6.

One of the strategies used to identify a reactive glial phenotype associated with the early phases of synucleinopathy in the SNpc was to quantify the expression of select genes that are upregulated in PD, AD or preclinical models of neurodegenerative disease. A subset of the genes analyzed via this strategy are associated with reactive astrocytes. Specifically, previous reports described how different pathological insults can convert resting astrocytes to a reactive phenotype. Specifically, ischemia converts astrocytes to a neuroprotective phenotype, dubbed “A2-astrocytes”, while cytokines released from microglia following LPS-induced neuroinflammation convert astrocytes to a neurotoxic phenotype, dubbed “A1-astrocytes”(Liddelow et al., 2017b; Zamanian et al., 2012). In their original description, these reactive astrocyte phenotypes were identified through a suite of genes specific to either the A1 or A2 phenotype, or genes upregulated in both A1 and A2 astrocytes, termed “pan-reactive genes”. In the current work we sought to determine if genes associated with these reactive astrocyte phenotypes were altered in the SNpc of PFF-injected rats. To this end we analyzed the expression of *C3, Serping1, Gbp2* and *Ggta1* (“A1” associated), *Emp1, S100a10, Tm4sf1* (“A2” associated), and *Osmr* (“pan” associated). Our results revealed a heterogeneous response, characterized by increases in genes associated with all 3 reactive phenotypes. This is not surprising as research continues to support the idea that reactive astrocytes do not fall into discrete binary classifications, such as A1 versus A2. Instead, the phenotype of reactive astrocytes is contextual, dictated by the type and severity of the initial insult, the time following the insult, and the brain region in which the glia reside (Escartin et al., 2021). Thus, the astrocyte associated genes upregulated in the current work

could be used to specifically describe a reactive phenotype unique to astrocytes in the rat SNpc during the early phases of synucleinopathy induced by α-syn PFFs. Nonetheless, it is informative that in our PFF model, which is characterized by neuroinflammation and subsequent neurodegeneration, the magnitude of upregulation of genes previously associated with the “neurotoxic A1” phenotype is far greater than the magnitude of upregulation of genes previously associated with the “neuroprotective A2” phenotype. This suggests that some of these genes (*C3, Gbp2, Serping1*) may indeed participate in a neurotoxic inflammatory response. However, future mechanistic studies examining the function of these gene products are necessary to unequivocally tie them to toxicity.

A limitation of the current work is that we did not confirm the astrocytic cell source of all upregulated astrocyte-associated genes. We quantified changes in reactive astrocyte-associated transcripts from tissue punches of the SN, which includes astrocytes along with other cell types (neurons, microglia, oligodendrocytes, etc.,). Thus, from the ddPCR gene expression analysis alone, it is impossible to provide cellular resolution to changes in gene expression. As much as possible we attempted to determine the cellular source of upregulated genes using in situ hybridization. However, for practical reasons it was not possible to perform this type of analysis for all genes analyzed by ddPCR. For example, we attempted to localize expression of some genes (such as *Gbp2*) butthe expression levels were below the limit of detection for FISH. It is therefore possible that some of the upregulated genes associated with astrocytes in the literature may be coming from an alternative, non-astrocytic cell type. An excellent example of this is the expression of *C3* in microglia at 2–4 months post-injection, which then shifts to astrocytes by 6 months post-injection. At 2-months post-PFF-injection, *C3* is one of the most highly upregulated genes we quantified in the SN of PFF-injected animals, and this is in line with previous reports that describe *C3* as one of the most consistently upregulated genes associated with reactive astrocytes in other animal models (Liddelow et al., 2017b). However, follow up analysis showed *C3* expression localized to microglia, not astrocytes, at the 2-month time point. These data once again highlight how context (including time from the initial insult) dictates the phenotype of reactive glia, and support the idea that reactive glia cannot be classified using a single metric (e.g. C3 expression). However, if one considers the timing of the degenerative cascade, the data presented here are consistent with previous reports. C3+ astrocytes are present in the SNpc of postmortem human PD tissue and α-syn PFF-injected mice after significant neurodegeneration has occurred (Liddelow et al., 2017b; Yun et al., 2018). Similarly, we observe *C3*+ astrocytes in the SNpc of PFF-injected rats after significant nigral neuron loss (i.e. 6-months post-injection). Interestingly, *C3* expression was still restricted to microglia at the 4-month time point, which is immediately prior to overt neurodegeneration. Taken together, these collective findings suggest that *C3*+ reactive astrocytes appear in response to cell death. It is possible that activated C3 released from astrocytes is used as an opsonin to tag cell debris and dead neurons for phagocytosis after neurodegeneration has occurred. However, future research is necessary to determine the function of C3 released from microglia versus astrocytes.

An important question that remains unanswered is how the switch in *C3* expression between microglia and astrocytes is coordinated. It is possible that C3 coordinates communication between astrocytes and microglia to modulate the production of inflammatory molecules

(such as C3 itself). Recent work using human pluripotent stem cell derived astrocyte-microglia co-cultures, describes a crosstalk between these two cell types that modulates a feedforward neuroinflammatory loop (Guttikonda et al., 2021). In this loop, C3 producing microglia initiate the inflammatory cascade and signal astrocytes to produce C3, which in turn reinforces microglia to produce more C3. In this system, C3 itself as well as TNF-α were identified as secreted molecules that mediate coordinated activity between microglia and astrocytes. Others have also reported C3-mediated crosstalk between microglia and astrocytes, a process involved in the neuroinflammatory response to β-amyloid and tau(Lian et al., 2016; Litvinchuk et al., 2018). Accordingly, it is possible that C3 produced in microglia stimulates astrocytic C3 expression at later time points. Taken together, the current work provides evidence that accumulation of α-syn inclusions can stimulate the conversion of homeostatic astrocytes to a reactive phenotype, and that C3 may coordinate the inflammatory response between microglia and astrocytes.

The second primary goal of this work was to identify a unique α-syn associated microglial gene expression signature. Under homeostatic conditions microglia are dynamic cells that continuously survey the microenvironment (Nimmerjahn et al., 2005). Upon encountering an activating stimulus (whether physiological or pathological), microglia undergo complex and dynamic morphologic, epigenetic, transcriptomic, proteomic, metabolic and functional changes (Paolicelli et al., 2022). Our previous work demonstrates that α-syn inclusions in the rat SNpc stimulate microglia to alter their morphology and express MHC-II (Duffy et al., 2018; Miller et al., 2021). In the present study, evaluation beyond microglial soma size and MHC-II expression was conducted to increase our understanding of gene expression changes in microglia responding to synucleinopathy in the rat SNpc. Our results identify a unique α-syn aggregate associated microglial gene expression profile, in which a subset of microglia in immediate proximity to α-syn inclusions upregulate *Cd74, Cxcl10, Rt1-a2, Grn, Tyrobp, Fger1g, Csf1r, Serping1, C3* and *C1qa* (Fig. 6). This gene expression profile of reactive microglia in the SNpc of PFF injected rats aligns with reactive microglial phenotypes observed in human neurodegenerative disease and associated models.

Recent transcriptomic studies have shed light on the complex and dynamic response of microglia to pathology associated with different neurodegenerative diseases. The emergent view suggests that while there is significant heterogeneity in reactive microglial phenotypes based on the type of initial insult, the brain region and many other factors (Paolicelli et al., 2022), microglia respond to insults by altering their transcriptional profile to transition from a homeostatic state into one of many possible reactive states, each characterized by a distinct gene expression signature. For example, single nuclei RNA sequencing (snRNA-Seq) of microglia isolated from the midbrain of idiopathic PD patients reveals transcriptomic signatures distinct from microglia isolated from age-matched healthy midbrains (Smajić et al., 2022b). PD microglia stratify into distinct states, the 4 largest of which are characterized by increased expression of either *P2RY12*, *GPNMB*, *HSP90AA1* or *IL1B* (Smajić et al., 2022b). Of the different states identified, the *P2RY12* group likely represents homeostatic microglia, while the other 3 subgroups represent distinct subsets of reactive microglia. Interestingly, microglia from PD midbrain exist on an activation trajectory, moving from the $P2RY12^{high}$ homeostatic subset to either the $HSP90AA1/IL1B^{high}$ or $GPNMB^{high}$ reactive subsets. Similarly, comparing the transcriptional profile of microglia isolated

from the midbrain of young, aged and PD individuals, reveals enrichment in *P2RY12*^{high} homeostatic microglial in the young midbrain, which shift towards reactive microglial clusters characterized by decreased *P2RY12* expression and increased *TYROBP*, *GRN* and *TREM2* expression in the aged and PD midbrain (Adams et al., 2022). Finally, spatial proteomic profiling of microglia in the AD brain reveals a similar pattern, where microglia in the immediate vicinity of amyloid plaques and tau tangles decrease expression of *P2RY12* and increase expression of *CD74* and *HLA-DR* (Mrdjen et al., 2023).

Currently, single cell and single nuclei transcriptomic studies in models of synucleinopathy are lacking, limiting the ability to compare results from the current study. One study performed snRNA-Seq on the midbrain and striatum of 6-month-old human A53T α-syn transgenic mice (Zhong et al., 2021). However, this analysis focused primarily on neuronal transcriptomic changes and found very few differentially expressed genes in microglia, likely due to the time selected (6 months) which is prior to the formation of α-syn inclusions (Giasson et al., 2002). In contrast, single cell (sc) RNA-Seq of microglia in the CK-p25 mouse model of neurodegeneration revealed a time dependent shift in microglial phenotypes, similar to that observed in human studies. Specifically, microglia isolated from young CK-p25 mice (prior to severe neurodegeneration) were distributed across distinct states that resembled microglia in the brains of healthy mice and were distinct from microglia isolated at later stages of neurodegeneration (Mathys et al., 2017b). Microglia isolated from aged CK-p25 mice (following neurodegeneration) increased expression of immune response genes such as *C3*, *Axl*, *Cd74*, MHC-1 genes, MHC-II genes and interferon response genes (Mathys et al., 2017b). Importantly, many of the genes that characterized the late response microglia were already increased in early response microglia, again supporting the notion of a gradual transition from a homeostatic to a specialized, reactive state with disease progression.

Taken together these results align with the unique suite of genes upregulated by microglia following α-syn inclusion accumulation induced by α-syn PFFs in the current study. Microglia in the immediate vicinity of α-syn inclusions upregulate *Cd74, Cxcl10, Rt1-a2, Grn, Tyrobp, Fger1g, Csf1r, Serping1, C3, C1qa* and MHC-II (similar to microglia in human disease and other models of neurodegeneration), supporting a shift towards a reactive phenotype. Unlike reactive microglia in human disease, we did not detect a decrease in *P2ry12* expression. As mentioned, the purinergic receptor P2RY12 is considered a marker of homeostatic microglia which is decreased in reactive microglia (Paolicelli et al., 2022). One possible reason we did not detect a decrease in *P2ry12* in the currents study is that we quantified *P2ry12* in whole SN punches (containing multiple cell types) using ddPCR. Thus, a decrease in *P2ry12* in microglia could be masked by expression in other cell types, however *P2ry12* expression in other non-microglial cell types of the CNS is low. Alternatively, the unchanged levels of *P2ry12* could reflect a heterogenous population of microglia in the SN of PFF injected rats. As mentioned, transcriptomic studies suggest microglia lie on an activation trajectory following an initial insult, characterized by a continual shift from *P2RY12*^{high} homeostatic microglia towards *P2RY12*^{low} reactive microglia (Adams et al., 2022; Mathys et al., 2017b; Smajić et al., 2022b). We intentionally aimed to characterize early neuroinflammatory changes in the current study, and as such there may be a mix of homeostatic and reactive microglia in the SN of PFF injected

rats at this early time point. Nonetheless, the current findings support the notion that synucleinopathy stimulates a heterogenous immune response broadly characterized by a shift towards a more reactive microglial population. Future studies utilizing more sophisticated sequencing technology will be necessary to characterize the distinct states of microglia (both homeostatic and reactive) that exist in the SN of PFF injected rats.

The current results contribute to a very large body of evidence supporting the conclusion that synucleinopathy stimulates the conversion of microglia to a reactive phenotype. However, an important question that remains is the precise nature by which pathological α-syn activates microglia in vivo. Extracellular wild type α-syn can directly activate microglia (as well as monocytes) in a concentration dependent manner, and this direct activation is dramatically increased by fibrillar forms of α-syn and α-syn containing familial-PD associated mutations (Grozdanov et al., 2019). α-syn activation of microglia is mediated, at least in part, by pattern recognition receptors, of which toll-like receptors (TLRs) have been garnering increased attention(Béraud and Maguire-Zeiss, 2012; Fellner et al., 2013; Kim et al., 2013, 2018; Stefanova et al., 2011). Activation of TLRs on microglia leads to morphological changes, increased indices of phagocytosis and increased production of proinflammatory cytokines (Fiebich et al., 2018; Heidari et al., 2022b), which are observed in PD and the rat PFF model (Chen et al., 2018; Duffy et al., 2018; McGeer et al., 1988; McGeer and McGeer, 2004; Qin et al., 2016; Zimmermann and Brockmann, 2022). Activation of microglia by α-syn also increases the expression of TLRs (Béraud and Maguire-Zeiss, 2012), and TLRs are increased in the PD brain and models of synucleinopathy (Heidari et al., 2022b; Kim et al., 2018). Finally, blocking the ability of α-syn to activate TLRs reduces microglial activation and subsequent neurodegeneration in models of synucleinopathy (Kim et al., 2013, 2018). These data suggest TLRs represent a primary signaling mechanism through which α-syn activates microglia, however, there are likely others. For example, MHC-II is also required microglial activation and neurodegeneration in models of synucleinopathy (Harm et al., 2013). Additionally, the Fcγ receptor and proteinase-activated receptor-1 have also been implicated in α-syn activation of microglia (Cao et al., 2012; Lee et al., 2010), suggesting multiple microglial receptors have the capacity to respond to extracellular α-syn. Regardless, the question of how microglia come into contact with α-syn in the current model remains. In the current study, recombinant α-syn PFFs were injected into the striatum, which is physically separated from the SNpc, and as such diffusion of the injectate from the striatum to the SNpc is improbable. Further, at this early time point we do not observe significant neurodegeneration (Patterson et al., 2019a), indicating α-syn is not being released for dead/dying neurons. It is possible that misfolded α-syn within nigral neurons is being released, potentially within extracellular vesicles, after which it is activating microglia (Kim et al., 2013). Indeed, α-syn released from neurons activates TLR2 (Kim et al., 2013), and α-syn within extracellular vesicles is a far more potent microglial stimulator than free extracellular α-syn (Grozdanov et al., 2019). This is an interesting and potentially important question that should be addressed in future experiments.

One limitation of the current study is the FISH approach limited the number of genes that could be colocalized within individual microglia and astrocytes. Thus, while we observe abundant co-expression of *Cxcl10, Rt1-a2, Grn, Tyrobp, Fger1g, Csf1r, Serping1 and C3* in *Cd74*+ microglia, it is currently unclear if all these genes are upregulated in the same

population of *Cd74*+ microglia, or if they are expressed in separate populations of *Cd74*+ microglia. Given the stratification of reactive microglia into distinct states characterized by unique transcriptomic profiles, this remains an important unanswered question. Further, we were unable to provide cellular localization for all upregulated genes identified by ddPCR. *Axl*, *Stat1*, *Casp1*, *Il18*, *Lyz2*, *Tm4sf1*, *Clcf1*, *Gbp2* and *Osmr* were significantly upregulated in the SN of PFF injected rats, but it is currently unclear which cells increased expression of these genes. We did attempt to identify the cellular source of some of these transcripts (e.g. *Gbp2*), however the expression levels were below the limit of detection by FISH. Many of these genes have previously been ascribed to reactive astrocytes (*Tm4sf1*, *Clcf1*, *Gbp2* and *Osmr* (Liddelow et al., 2017b)), while others have been associated with reactive microglia (*Axl, Stat1, Lyz2, IL18, Casp1* (Anderson et al., 2019; Hanslik and Ulland, 2020; Mathys et al., 2017b; Przanowski et al., 2014; Scheiblich et al., 2021; Zhao et al., 2022)). However, as this study and others has illustrated, the gene expression phenotype of reactive glia is highly contextual, and more work is needed to unequivocally determine the cellular source of these immune associated transcripts. In contrast, the upregulated genes that were localized to microglia in the SNpc of PFF injected rats shed light onto the possible effector functions adopted by reactive microglia in response to α-syn inclusion accumulation in the rat SNpc. The major immune pathways implicated by the upregulated genes are phagocytosis (*Fcer1g*, *Grn*), antigen presentation and T-cell regulation (*Cd74*, *Rt1-a2*), complement activation (*C1qa*, *C3*) and cytokine/chemokine signaling (*Tyrobp, Grn, Cxcl10*). These biological processes are all increased in the brains and periphery of PD patients (Cebrián et al., 2014; Chen et al., 2018; Lindestam Arlehamn et al., 2020; Loeffler et al., 2006; McGeer et al., 1988; Qin et al., 2016; Sulzer et al., 2017; Yamada et al., 1992; Zhang and Gao, 2022; Zimmermann and Brockmann, 2022), providing further support that the microglial response to synucleinopathy may contribute to PD pathogenesis. However, inferring a functional phenotype solely from gene expression changes should be undertaken with caution, and future mechanistic studies are necessary to conclusively characterize the functional phenotype of reactive microglial in the SN of PFF injected rats.

Finally, the current work also demonstrates *Rt1-a2* expression in TH+ nigral neurons. As mentioned, *Rt1-a2* encodes a portion of the MHC-1 complex. Nigral dopamine neurons, as well as locus coeruleus noradrenergic neurons, in the PD brain express MHC-1 (Cebrián et al., 2014). In this work, Cebrián et al. (2014) also reported induction of MHC-1 expression in primary murine ventral midbrain DA neurons following exposure to interferon gamma or conditioned medium taken from microglia treated with α-syn. Accordingly, it is possible that in the current study, nigral DA neuron *Rt1-a2* expression was induced by cytokines released from activated microglia following synucleinopathy. However, this is unlikely as we observed *Rt1-a2* expression in TH+ neurons in both the ipsilateral and contralateral SNpc of PFF injected rats. At this early time point, the contralateral SNpc is unaffected by synucleinopathy and devoid of indices of microglia activation. As such, the expression of *Rt1-a2* by the majority of TH+ neurons in the contralateral SNpc suggest nigral DA neurons may express *Rt1-a2* under physiological conditions. Further analysis is needed to confirm this supposition. For example, do TH+ neurons in naïve animals also express *Rt1a-2*? It should be noted that *Rt1-a2* expression is increased in the ipsilateral SNpc of PFF injected rats. However, this increased expression is likely occurring in reactive microglia,

as we were able to localize increased *Rt1-a2* mRNA to Iba1+/*Cd74*+ microglia in the synucleinopathy affected SNpc. Nonetheless, the current findings could explain why nigral dopamine neurons appear to be particularly susceptible to T-cell mediated attack. Primary murine catecholamine neurons are more responsive to MHC-1 induction by interferon gamma than other neuronal populations (Cebrián et al., 2014). If nigral dopamine neurons express *Rt1-a2* under physiological conditions, they may be primed for a faster and larger induction of MHC-1 expression than other neurons, which could in turn render them vulnerable to attack by cytotoxic T-cells. Future work is needed to determine if the *Rt1-a2* transcript is translated to produce a functional MHC-1 complex in nigral dopamine neurons, and if this a physiological process or solely occurs in response to a pathological insult.

Overall, our results demonstrate the heterogeneity of inflammatory responses, associated with both microglia and astrocytes, to α-syn aggregates in the SNpc. The inflammatory responses present as a complex network of interconnecting functional pathways mediated by multiple cell types (Supplemental Fig. 3D). An important lesson from this work is that there is a large degree of functional crossover between astrocytes and microglia. As such, attempting to profile a single cell type through a single function may be misleading and should be avoided. Future studies that provide a more comprehensive and nuanced understanding of the neuroinflammatory signature of glia associated with pathological α-syn aggregates will be needed to facilitate future investigation of anti-inflammatory, disease-modifying approaches for PD.

5. Conclusions

We identified a suite of immune genes that are upregulated in the SN during the early phases of synucleinopathy, including *Cd74*, *C1qa*, *Stat1, Axl, Casp1, Il18, Lyz2, C3, Gbp2, Serping1*. Using FISH to identify the cellular source of upregulated genes, we identified an α-syn aggregate microglial gene expression profile characterized by upregulation of *Cd74, Cxcl10, Rt-1a2, Grn, Csf1r, Tyrobp, Serping1, C3, C1qa* and *Fcer1g* in microglia near α-syn aggregates in the rat SNpc. FISH localization of complement *C3* expression in the SNpc revealed a cell type switching between microglia and astrocytes over the degenerative cascade, where microglia are the primary cellular source of *C3* expression prior to nigral dopamine neuron neurodegeneration, but astrocytes are the primary cellular source of *C3* following degeneration. Finally, we also observed *Rt1-a2* expression in SNpc dopamine neurons in both the ipsilateral (injected) and contralateral (naïve) hemispheres, suggesting nigral dopamine neurons may express *Rt-1a2* physiologically. Overall, our results identify a dynamic and reproducible gene expression profile of reactive glia associated with early synucleinopathy in the SNpc.

Supplementary Material

Refer to Web version on PubMed Central for supplementary material.

Acknowledgements

Support was provided by National Institutes of Health (NS111333 and NS099416 to CES, NS121393 to MJB) and the MSU Integrative Pharmacological Sciences Training Program T32GM092715.

Funding

Support was provided by National Institutes of Health (NS111333 to CES, NS121393 to MJB) and the MSU Integrative Pharmacological Sciences Training Program T32GM092715.

Declaration of competing interest

CES receives funding from Takeda, Inc. All remaining authors declare they have no competing interests.

Data availability

Data will be made available on request.

References

Adams L, Kyung Song M, Tanaka Y, Kim Y-S, 2022. Single-nuclei paired multiomic analysis of young, aged, and Parkinson's disease human midbrain reveals age-associated glial changes and their contribution to Parkinson's disease. medRxiv. 10.1101/2022.01.18.22269350.

Ahmadi Rastegar D, Ho N, Halliday GM, Dzamko N, 2019. Parkinson's progression prediction using machine learning and serum cytokines. NPJ Parkinsons Dis. 5 10.1038/s41531-019-0086-4.

Anderson SR, Roberts JM, Zhang J, Steele MR, Romero CO, Bosco A, Vetter ML, 2019. Developmental apoptosis promotes a disease-related gene signature and Independence from CSF1R signaling in retinal microglia. Cell Rep. 27, 2002–2013. e5. 10.1016/j.celrep.2019.04.062. [PubMed: 31091440]

Barnum CJ, Tansey MG, 2010. Modeling Neuroinflammatory Pathogenesis of Parkinson's Disease, Progress in Brain Research. Elsevier B.V. 10.1016/S0079-6123(10)84006-3.

Benskey MJ, Sellnow RC, Sandoval IM, Sortwell CE, Lipton JW, Manfredsson FP, 2018. Silencing alpha synuclein in mature nigral neurons results in rapid neuroinflammation and subsequent toxicity. Front. Mol. Neurosci 11 10.3389/fnmol.2018.00036.

Béraud D, Maguire-Zeiss KA, 2012. Misfolded α-synuclein and toll-like receptors: therapeutic targets for Parkinson's disease. Parkinsonism Relat. Disord 18, S17–S20. 10.1016/S1353-8020(11)70008-6. [PubMed: 22166424]

Bettcher BM, Tansey MG, Dorothée G, Heneka MT, 2021. Peripheral and central immune system crosstalk in Alzheimer disease — a research prospectus. Nat. Rev. Neurol 17, 689–701. 10.1038/s41582-021-00549-x. [PubMed: 34522039]

Blum-Degena D, Müller T, Kuhn W, Gerlach M, Przuntek H, Riederer P, 1995. Interleukin-1β and interleukin-6 are elevated in the cerebrospinal fluid of Alzheimer's and de novo Parkinson's disease patients. Neurosci. Lett 202, 17–20. 10.1016/0304-3940(95)12192-7. [PubMed: 8787820]

Boche D, Gordon MN, 2022. Diversity of transcriptomic microglial phenotypes in aging and Alzheimer's disease. Alzheimers Dement. 18, 360–376. 10.1002/alz.12389. [PubMed: 34223696]

Brodacki B, Staszewski J, Toczyłowska B, Kozłowska E, Drela N, Chalimoniuk M, Stepien A, 2008. Serum interleukin (IL-2, IL-10, IL-6, IL-4), TNFα, and INFγ concentrations are elevated in patients with atypical and idiopathic parkinsonism. Neurosci. Lett 441, 158–162. 10.1016/j.neulet.2008.06.040. [PubMed: 18582534]

Burda JE, Sofroniew MV, 2014. Reactive gliosis and the multicellular response to CNS damage and disease. Neuron. 10.1016/j.neuron.2013.12.034.

Cao S, Standaert DG, Harms AS, 2012. The gamma chain subunit of fc receptors is required for alpha-synuclein-induced pro-inflammatory signaling in microglia. J. Neuroinflamm 9, 259. 10.1186/1742-2094-9-259.

Cebrián C, Zucca FA, Mauri P, Steinbeck JA, Studer L, Scherzer CR, Kanter E, Budhu S, Mandelbaum J, Vonsattel JP, Zecca L, Loike JD, Sulzer D, 2014. MHC-I expression renders catecholaminergic neurons susceptible to T-cell-mediated degeneration. Nat. Commun 5 10.1038/ncomms4633.

Chen H, Jacobs E, Schwarzschild MA, McCullough ML, Calle EE, Thun MJ, Ascherio A, 2005. Nonsteroidal antiinflammatory drug use and the risk for Parkinson's disease. Ann. Neurol 58, 963–967. 10.1002/ana.20682. [PubMed: 16240369]

Chen H, Zhang SM, Hernán MA, Schwarzschild MA, Willett WC, Colditz GA, Speizer FE, Ascherio A, n.d. Nonsteroidal Anti-inflammatory Drugs and the Risk of Parkinson Disease.

Chen X, Hu Y, Cao Z, Liu Q, Cheng Y, 2018. Cerebrospinal fluid inflammatory cytokine aberrations in Alzheimer's disease, Parkinson's disease and amyotrophic lateral sclerosis: a systematic review and meta-analysis. Front. Immunol 10.3389/fimmu.2018.02122.

Chen Y, Colonna M, 2021. Microglia in Alzheimer's disease at single-cell level. Are there common patterns in humans and mice? J. Exp. Med 218 10.1084/jem.20202717.

Compta Y, Dias SP, Giraldo DM, Pérez-Soriano A, Muñoz E, Saura J, Fernández M, Bravo P, Cámara A, Pulido-Salgado M, Painous C, Ríos J, Martí MJ, Pagonabarraga J, Valldeoriola F, Hernández-Vara J, Classen SJ, Puente V, Pont C, Caballol N, Tolosa E, Bayes A, Campdelacreu J, de Fàbregues O, Ávila A, Calopa M, Gaig C, Fabregat N, Pastor P, Aguilar M, Pujol M, Sánchez A, Planellas L, Ezquerra M, Fernández-Santiago R, Botta T, Tartaglia G, 2019. Cerebrospinal fluid cytokines in multiple system atrophy: a cross-sectional Catalan MSA registry study. Parkinsonism Relat. Disord 65, 3–12. 10.1016/j.parkreldis.2019.05.040. [PubMed: 31178335]

Croisier E, Moran LB, Dexter DT, Pearce RKB, Graeber MB, 2005. Microglial inflammation in the parkinsonian substantia nigra: relationship to alpha-synuclein deposition. J. Neuroinflammation 2. 10.1186/1742-2094-2-14.

Deczkowska A, Keren-Shaul H, Weiner A, Colonna M, Schwartz M, Amit I, 2018. Disease-associated microglia: a universal immune sensor of neurodegeneration. Cell 173, 1073–1081. 10.1016/j.cell.2018.05.003. [PubMed: 29775591]

Dijkstra AA, Ingrassia A, De Menezes RX, Van Kesteren RE, Rozemuller AJM, Heutink P, Van De Berg WDJ, 2015. Evidence for immune response, axonal dysfunction and reduced endocytosis in the substantia nigra in early stage Parkinson's disease. PLoS One 10. 10.1371/journal.pone.0128651.

Dubbelaar ML, Kracht L, Eggen BJL, Boddeke EWGM, 2018. The kaleidoscope of microglial phenotypes. Front. Immunol 9 10.3389/fimmu.2018.01753.

Duffy MF, Collier TJ, Patterson JR, Kemp CJ, Luk KC, Tansey MG, Paumier KL, Kanaan NM, Fischer LD, Polinski NK, Barth OL, Howe JW, Vaikath NN, Majbour NK, El-Agnaf OMA, Sortwell CE, 2018. Lewy body-like alpha-synuclein inclusions trigger reactive microgliosis prior to nigral degeneration. J. Neuroinflammation 15. 10.1186/s12974-018-1171-z.

Escartin C, Galea E, Lakatos A, O'Callaghan JP, Petzold GC, Serrano-Pozo A, Steinhäuser C, Volterra A, Carmignoto G, Agarwal A, Allen NJ, Araque A, Barbeito L, Barzilai A, Bergles DE, Bonvento G, Butt AM, Chen WT, Cohen-Salmon M, Cunningham C, Deneen B, De Strooper B, Díaz-Castro B, Farina C, Freeman M, Gallo V, Goldman JE, Goldman SA, Götz M, Gutiérrez A, Haydon PG, Heiland DH, Hol EM, Holt MG, Iino M, Kastanenka KV, Kettenmann H, Khakh BS, Koizumi S, Lee CJ, Liddelow SA, MacVicar BA, Magistretti P, Messing A, Mishra A, Molofsky AV, Murai KK, Norris CM, Okada S, Oliet SHR, Oliveira JF, Panatier A, Parpura V, Pekna M, Pekny M, Pellerin L, Perea G, Pérez-Nievas BG, Pfrieger FW, Poskanzer KE, Quintana FJ, Ransohoff RM, Riquelme-Perez M, Robel S, Rose CR, Rothstein JD, Rouach N, Rowitch DH, Semyanov A, Sirko S, Sontheimer H, Swanson RA, Vitorica J, Wanner IB, Wood LB, Wu J, Zheng B, Zimmer ER, Zorec R, Sofroniew MV, Verkhratsky A, 2021. Reactive astrocyte nomenclature, definitions, and future directions. Nat. Neurosci 24, 312–325. 10.1038/s41593-020-00783-4. [PubMed: 33589835]

Fellner L, Irschick R, Schanda K, Reindl M, Klimaschewski L, Poewe W, Wenning GK, Stefanova N, 2013. Toll-like receptor 4 is required for α-synuclein dependent activation of microglia and astroglia. Glia 61, 349–360. 10.1002/glia.22437. [PubMed: 23108585]

Fiebich BL, Batista CRA, Saliba SW, Yousif NM, de Oliveira ACP, 2018. Role of microglia TLRs in neurodegeneration. Front. Cell. Neurosci 12 10.3389/fncel.2018.00329.

Gao X, Chen H, Schwarzschild MA, Ascherio A, 2011. Use of Ibuprofen and Risk of Parkinson Disease.

Gate D, Tapp E, Leventhal O, Shahid M, Nonninger TJ, Yang AC, Strempfl K, Unger MS, Fehlmann T, Oh H, Channappa D, Henderson VW, Keller A, Aigner L, Galasko DR, Davis MM, Poston KL, Wyss-Coray T, 2021. CD4 $^{+}$ T cells contribute to neurodegeneration in Lewy body dementia. Science 1979 (374), 868–874. 10.1126/science.abf7266.

Gerhard A, Pavese N, Hotton G, Turkheimer F, Es M, Hammers A, Eggert K, Oertel W, Banati RB, Brooks DJ, 2006. In vivo imaging of microglial activation with [11C](R)-PK11195 PET in

idiopathic Parkinson's disease. Neurobiol. Dis 21, 404–412. 10.1016/j.nbd.2005.08.002. [PubMed: 16182554]

Giasson BI, Duda JE, Quinn SM, Zhang B, Trojanowski JQ, M-Y Lee V, 2002. Neuronal-synucleinopathy with severe movement disorder in mice expressing A53T human-synuclein. Neuron. 34 (4), 521–533. 10.1016/s0896-6273(02)00682-7. [PubMed: 12062037]

Grozdanov V, Bousset L, Hoffmeister M, Bliederhaeuser C, Meier C, Madiona K, Pieri L, Kiechle M, McLean PJ, Kassubek J, Behrends C, Ludolph AC, Weishaupt JH, Melki R, Danzer KM, 2019. Increased immune activation by pathologic α-Synuclein in Parkinson's disease. Ann. Neurol 86, 593–606. 10.1002/ana.25557. [PubMed: 31343083]

Guttikonda SR, Sikkema L, Tchieu J, Saurat N, Walsh RM, Harschnitz O, Ciceri G, Sneeboer M, Mazutis L, Setty M, Zumbo P, Betel D, de Witte LD, Pe'er D, Studer L, 2021. Fully defined human pluripotent stem cell-derived microglia and tri-culture system model C3 production in Alzheimer's disease. Nat. Neurosci 24, 343–354. 10.1038/s41593-020-00796-z. [PubMed: 33558694]

Hamza TH, Zabetian CP, Tenesa A, Laederach A, Montimurro J, Yearout D, Kay DM, Doheny KF, Paschall J, Pugh E, Kusel VI, Collura R, Roberts J, Griffith A, Samii A, Scott WK, Nutt J, Factor SA, Payami H, 2010. Common genetic variation in the HLA region is associated with late-onset sporadic Parkinson's disease. Nat. Genet 42, 781. 10.1038/ng.642. [PubMed: 20711177]

Hanslik KL, Ulland TK, 2020. The role of microglia and the Nlrp3 inflammasome in Alzheimer's disease. Front. Neurol 10.3389/fneur.2020.570711.

Harm AS, Cao S, Rowse AL, Thome AD, Li X, Mangieri LR, Cron RQ, Shacka JJ, Raman C, Standaert DG, 2013. MHCII is required for α-Synuclein-induced activation of microglia, CD4 T cell proliferation, and dopaminergic neurodegeneration. J. Neurosci 33, 9592–9600. 10.1523/JNEUROSCI.5610-12.2013. [PubMed: 23739956]

Hasel P, Aisenberg WH, Bennett FC, Liddelow SA, 2023. Molecular and metabolic heterogeneity of astrocytes and microglia. Cell Metab. 10.1016/j.cmet.2023.03.006.

Heidari A, Yazdanpanah N, Rezaei N, 2022a. The role of toll-like receptors and neuroinflammation in Parkinson's disease. J. Neuroinflammation 19, 135. 10.1186/s12974-022-02496-w. [PubMed: 35668422]

Heidari A, Yazdanpanah N, Rezaei N, 2022b. The role of toll-like receptors and neuroinflammation in Parkinson's disease. J. Neuroinflammation 10.1186/s12974-022-02496-w.

Helmfors L, Boman A, Civitelli L, Nath S, Sandin L, Janefjord C, McCann H, Zetterberg H, Blennow K, Halliday G, Brorsson A-C, Kågedal K, 2015. Protective properties of lysozyme on β-amyloid pathology: implications for Alzheimer disease. Neurobiol. Dis 83, 122–133. 10.1016/j.nbd.2015.08.024. [PubMed: 26334479]

van Hove H, Martens L, Scheyltjens I, de Vlaminck K, Pombo Antunes AR, de Prijck S, Vandamme N, de Schepper S, van Isterdael G, Scott CL, Aerts J, Berx G, Boeckxstaens GE, Vandenbroucke RE, Vereecke L, Moechars D, Guilliams M, van Ginderachter JA, Saeys Y, Movahedi K, 2019. A single-cell atlas of mouse brain macrophages reveals unique transcriptional identities shaped by ontogeny and tissue environment. Nat. Neurosci 22, 1021–1035. 10.1038/s41593-019-0393-4. [PubMed: 31061494]

Imamura K, Hishikawa N, Sawada M, Nagatsu T, Yoshida M, Hashizume Y, 2003. Distribution of major histocompatibility complex class II-positive microglia and cytokine profile of Parkinson's disease brains. Acta Neuropathol. 106, 518–526. 10.1007/s00401-003-0766-2. [PubMed: 14513261]

Jensen PE, Weber DA, Thayer WP, Chen X, Dao CT, 1999. HLA-DM and the MHC class II antigen presentation pathway. Immunol. Res 20, 195–205. 10.1007/BF02790403. [PubMed: 10741860]

Karpenko MN, Vasilishina AA, Gromova EA, Muruzheva ZM, Bernadotte A, 2018. Interleukin-1β interleukin-1 receptor antagonist, interleukin-6, interleukin-10, and tumor necrosis factor-α levels in CSF and serum in relation to the clinical diversity of Parkinson's disease. Cell. Immunol 327, 77–82. 10.1016/j.cellimm.2018.02.011. [PubMed: 29478949]

Keren-Shaul H, Spinrad A, Weiner A, Matcovitch-Natan O, Dvir-Szternfeld R, Ulland TK, David E, Baruch K, Lara-Astaiso D, Toth B, Itzkovitz S, Colonna M, Schwartz M, Amit I, 2017. A unique microglia type associated with restricting development of Alzheimer's disease. Cell 169, 1276–1290.e17. 10.1016/j.cell.2017.05.018. [PubMed: 28602351]

Kim C, Ho DH, Suk JE, You S, Michael S, Kang J, Lee Sung Joong, Masliah E, Hwang D, Lee HJ, Lee Seung Jae, 2013. Neuron-released oligomeric α-synuclein is an endogenous agonist of TLR2 for paracrine activation of microglia. Nat. Commun 4 10.1038/ncomms2534.

Kim C, Spencer B, Rockenstein E, Yamakado H, Mante M, Adame A, Fields JA, Masliah D, Iba M, Lee HJ, Rissman RA, Lee SJ, Masliah E, 2018. Immunotherapy targeting toll-like receptor 2 alleviates neurodegeneration in models of synucleinopathy by modulating α-synuclein transmission and neuroinflammation. Mol. Neurodegener 13 10.1186/s13024-018-0276-2.

Kübler D, Wächter T, Cabanel N, Su Z, Turkheimer FE, Dodel R, Brooks DJ, Oertel WH, Gerhard A, 2019. Widespread microglial activation in multiple system atrophy. Mov. Disord 34, 564–568. 10.1002/mds.27620. [PubMed: 30726574]

Lavisse S, Goutal S, Wimberley C, Tonietto M, Bottlaender M, Gervais P, Kuhnast B, Peyronneau MA, Barret O, Lagarde J, Sarazin M, Hantraye P, Thiriez C, Remy P, 2021. Increased microglial activation in patients with Parkinson disease using [18F]-DPA714 TSPO PET imaging. Parkinsonism Relat. Disord 82, 29–36. 10.1016/j.parkreldis.2020.11.011. [PubMed: 33242662]

Lee E-J, Woo M-S, Moon P-G, Baek M-C, Choi I-Y, Kim W-K, Junn E, Kim H-S, 2010. α-Synuclein activates microglia by inducing the expressions of matrix metalloproteinases and the subsequent activation of protease-activated Receptor-1. J. Immunol 185, 615–623. 10.4049/jimmunol.0903480. [PubMed: 20511551]

Leys C, Ley C, Klein O, Bernard P, Licata L, 2013. Detecting outliers: do notuse standard deviation around the mean, use absolute deviation aroundthe median. J. Exp. Soc. Psychol 10.1016/j.jesp.2013.03.013.

Lian H, Litvinchuk A, Chiang ACA, Aithmitti N, Jankowsky JL, Zheng H, 2016. Astrocyte-microglia cross talk through complement activation modulates amyloid pathology in mouse models of alzheimer's disease. J. Neurosci 36, 577–589. 10.1523/JNEUROSCI.2117-15.2016. [PubMed: 26758846]

Liddelow SA, Guttenplan KA, Clarke LE, Bennett FC, Bohlen CJ, Schirmer L, Bennett ML, Münch AE, Chung WS, Peterson TC, Wilton DK, Frouin A, Napier BA, Panicker N, Kumar M, Buckwalter MS, Rowitch DH, Dawson VL, Dawson TM, Stevens B, Barres BA, 2017a. Neurotoxic reactive astrocytes are induced by activated microglia. Nature 541, 481–487. 10.1038/nature21029. [PubMed: 28099414]

Liddelow SA, Guttenplan KA, Clarke LE, Bennett FC, Bohlen CJ, Schirmer L, Bennett ML, Münch AE, Chung WS, Peterson TC, Wilton DK, Frouin A, Napier BA, Panicker N, Kumar M, Buckwalter MS, Rowitch DH, Dawson VL, Dawson TM, Stevens B, Barres BA, 2017b. Neurotoxic reactive astrocytes are induced by activated microglia. Nature 541, 481–487. 10.1038/nature21029. [PubMed: 28099414]

Liddelow SA, Marsh SE, Stevens B, 2020. Microglia and astrocytes in disease: dynamic duo or Partners in Crime? Trends Immunol. 41, 820–835. 10.1016/j.it.2020.07.006. [PubMed: 32819809]

Lindestam Arlehamn CS, Dhanwani R, Pham J, Kuan R, Frazier A, Rezende Dutra J, Phillips E, Mallal S, Roederer M, Marder KS, Amara AW, Standaert DG, Goldman JG, Litvan I, Peters B, Sulzer D, Sette A, 2020. α-Synuclein-specific T cell reactivity is associated with preclinical and early Parkinson's disease. Nat. Commun 11 10.1038/s41467-020-15626-w.

Litvinchuk A, Wan YW, Swartzlander DB, Chen F, Cole A, Propson NE, Wang Q, Zhang B, Liu Z, Zheng H, 2018. Complement C3aR inactivation attenuates tau pathology and reverses an immune network deregulated in Tauopathy models and Alzheimer's disease. Neuron 100, 1337–1353.e5. 10.1016/j.neuron.2018.10.031. [PubMed: 30415998]

Liu SY, Qiao HW, Song T. Bin, Liu XL, Yao YX, Zhao CS, Barret O, Xu SL, Cai YN, Tamagnan GD, Sossi V, Lu J, Chan P, 2022. Brain microglia activation and peripheral adaptive immunity in Parkinson's disease: a multimodal PET study. J. Neuroinflammation 19. 10.1186/s12974-022-02574-z.

Loeffler DA, Camp DM, Conant SB, 2006. Complement activation in the Parkinson's disease substantia nigra: An immunocytochemical study. J. Neuroinflammation 3. 10.1186/1742-2094-3-29.

Luk KC, Kehm VM, Zhang B, O'Brien P, Trojanowski JQ, Lee VMY, 2012. Intracerebral inoculation of pathological α-synuclein initiates a rapidly progressive neurodegenerative α-synucleinopathy in mice. J. Exp. Med 209, 975–988. 10.1084/jem.20112457. [PubMed: 22508839]

Mathys H, Adaikkan C, Gao F, Young JZ, Manet E, Hemberg M, De Jager PL, Ransohoff RM, Regev A, Tsai L-H, 2017a. Temporal tracking of microglia activation in neurodegeneration at single-cell resolution. Cell Rep. 21, 366–380. 10.1016/j.celrep.2017.09.039. [PubMed: 29020624]

Mathys H, Adaikkan C, Gao F, Young JZ, Manet E, Hemberg M, De Jager PL, Ransohoff RM, Regev A, Tsai LH, 2017b. Temporal tracking of microglia activation in neurodegeneration at single-cell resolution. Cell Rep. 21, 366–380. 10.1016/j.celrep.2017.09.039. [PubMed: 29020624]

McGeer PL, McGeer EG, 2004. Inflammation and Neurodegeneration in Parkinson's Disease, in: Parkinsonism and Related Disorders. Elsevier BV, p. S3. 10.1016/j.parkreldis.2004.01.005.

McGeer PL, Itagaki S, Boyes BE, McGeer EG, 1988. Reactive microglia are positive for HLA-DR in the substantia nigra of Parkinsons and Alzheimers disease brains. Neurology 38, 1285. 10.1212/WNL.38.8.1285. [PubMed: 3399080]

Miller KM, Patterson JR, Kochmanski J, Kemp CJ, Stoll AC, Onyekpe CU, Cole-Strauss A, Steece-Collier K, Howe JW, Luk KC, Sortwell CE, 2021. Striatal afferent bdnf is disrupted by synucleinopathy and partially restored by stn dbs. J. Neurosci 41, 2039–2052. 10.1523/JNEUROSCI.1952-20.2020. [PubMed: 33472823]

Mogi M, Harada M, Kondo T, Riederer P, Inagaki H, Minami M, Nagatsu ET, 1994a. Interleukin-lfl, interleukin-6, epidermal growth factor and transforming growth factor-are elevated in the brain from parkinsonian patients. Neurosci. Lett 180, 147–150. [PubMed: 7700568]

Mogi M, Harada M, Riederer P, Narabayashi H, Fujita K, Nagatsu T, 1994b. Tumor necrosis factor-α (TNF-α) increases both in the brain and in the cerebrospinal fluid from parkinsonian patients. Neurosci. Lett 165, 208–210. 10.1016/0304-3940(94)90746-3. [PubMed: 8015728]

Mogi M, Harada M, Narabayashi H, Inagaki H, Minami M, Nagatsu T, 1996. Interleukin (IL)-lfl, IL-2, IL-4, IL-6 and transforming growth factor-a levels are elevated in ventricular cerebrospinal fluid in juvenile parkinsonism and Parkinson's disease. Neurosci. Lett 211, 13–16. [PubMed: 8809836]

Morgan DG, Mielke MM, 2021. Knowledge gaps in Alzheimer's disease immune biomarker research. Alzheimers Dement. 17, 2030–2042. 10.1002/alz.12342. [PubMed: 33984178]

Mrdjen D, Amouzgar M, Cannon B, Liu C, Spence A, McCaffrey E, Bharadwaj A, Tebaykin D, Bukhari S, Hartmann FJ, Kagel A, Vijayaragavan K, Oliveria JP, Yakabi K, Serrano GE, Corrada MM, Kawas CH, Camacho C, Bosse M, Tibshirani R, Beach TG, Angelo M, Montine T, Bendall SC, 2023. Spatial proteomics reveals human microglial states shaped by anatomy and neuropathology. Res. Sq 10.21203/rs.3.rs-2987263/v1.

Müller T, Blum-Degen D, Przuntek H, Kuhn W, 1998. Interleukin-6 levels in cerebrospinal fluid inversely correlate to severity of Parkinson's disease. Acta Neurol. Scand 98, 142–144. 10.1111/j.1600-0404.1998.tb01736.x. [PubMed: 9724016]

Nimmerjahn A, Kirchhoff F, Helmchen F, 2005. Resting microglial cells are highly dynamic Surveillants of brain parenchyma in vivo. Science 1979 (308), 1314–1318. 10.1126/science.1110647.

Orr CF, Rowe DB, Mizuno Y, Mori H, Halliday GM, 2005. A possible role for humoral immunity in the pathogenesis of Parkinson's disease. Brain 128, 2665–2674. 10.1093/brain/awh625. [PubMed: 16219675]

Ouchi Y, Yoshikawa E, Sekine Y, Futatsubashi M, Kanno T, Ogusu T, Torizuka T, 2005. Microglial activation and dopamine terminal loss in early Parkinson's disease. Ann. Neurol 57, 168–175. 10.1002/ana.20338. [PubMed: 15668962]

Paolicelli RC, Sierra A, Stevens B, Tremblay M-E, Aguzzi A, Ajami B, Amit I, Audinat E, Bechmann I, Bennett M, Bennett F, Bessis A, Biber K, Bilbo S, Blurton-Jones M, Boddeke E, Brites D, Brône B, Brown GC, Butovsky O, Carson MJ, Castellano B, Colonna M, Cowley SA, Cunningham C, Davalos D, De Jager PL, de Strooper B, Denes A, Eggen BJL, Eyo U, Galea E, Garel S, Ginhoux F, Glass CK, Gokce O, Gomez-Nicola D, González B, Gordon S, Graeber MB, Greenhalgh AD, Gressens P, Greter M, Gutmann DH, Haass C, Heneka MT, Heppner FL, Hong S, Hume DA, Jung S, Kettenmann H, Kipnis J, Koyama R, Lemke G, Lynch M, Majewska A, Malcangio M, Malm T, Mancuso R, Masuda T, Matteoli M, McColl BW, Miron VE, Molofsky AV, Monje M, Mracsko E, Nadjar A, Neher JJ, Neniskyte U, Neumann H, Noda M, Peng B, Peri F, Perry VH, Popovich PG, Pridans C, Priller J, Prinz M, Ragozzino D, Ransohoff RM, Salter MW, Schaefer A, Schafer DP, Schwartz M, Simons M, Smith CJ, Streit WJ, Tay TL, Tsai L-H, Verkhratsky A, von Bernhardi R, Wake H, Wittamer V, Wolf SA, Wu L-J, Wyss-Coray T, 2022. Microglia states and

nomenclature: a field at its crossroads. Neuron 110, 3458–3483. 10.1016/j.neuron.2022.10.020. [PubMed: 36327895]

Park S, Kim J, Chun J, Han K, Soh H, Kang EA, Lee HJ, Im JP, Kim JS, 2019. Patients with inflammatory bowel disease are at an increased risk of parkinson's disease: a south Korean nationwide population-based study. J. Clin. Med 8 10.3390/jcm8081191.

Patterson JR, Duffy MF, Kemp CJ, Howe JW, Collier TJ, Stoll AC, Miller KM, Patel P, Levine N, Moore DJ, Luk KC, Fleming SM, Kanaan NM, Paumier KL, El-Agnaf OMA, Sortwell CE, 2019a. Time course and magnitude of alpha-synuclein inclusion formation and nigrostriatal degeneration in the rat model of synucleinopathy triggered by intrastriatal α-synuclein preformed fibrils. Neurobiol. Dis 130 10.1016/j.nbd.2019.104525.

Patterson J, Kochmanski J, Stoll A, Kubik M, Kemp C, Duffy M, Thompson K, Howe J, Cole-Strauss A, Kuhn N, Miller K, Nelson S, Onyekpe C, Beck J, Counts S, Bernstein A, Steece-Collier K, Luk KC, Sortwell CE, 2024. Transcriptomic profiling of early Synucleinopathy in rats induced with preformed fibrils. NPJ Parkinsons Dis. 10.1038/s41531-023-00620-y.

Patterson JR, Polinski NK, Duffy MF, Kemp CJ, Luk KC, Volpicelli-Daley LA, Kanaan NM, Sortwell CE, 2019b. Generation of alpha-Synuclein preformed fibrils from monomers and use in vivo. J. Vis. Exp 10.3791/59758.

Patterson JR, Hirst WD, Howe JW, Russell CP, Cole-Strauss A, Kemp CJ, Duffy MF, Lamp J, Umstead A, Kubik M, Stoll AC, Vega IE, Steece-Collier K, Chen Y, Campbell AC, Nezich CL, Glajch KE, Sortwell CE, 2022. Beta2-adrenoreceptor agonist clenbuterol produces transient decreases in alpha-synuclein mRNA but no long-term reduction in protein. NPJ Parkinsons Dis. 8, 61. 10.1038/s41531-022-00322-x. [PubMed: 35610264]

Paumier KL, Luk KC, Manfredsson FP, Kanaan NM, Lipton JW, Collier TJ, Steece-Collier K, Kemp CJ, Celano S, Schulz E, Sandoval IM, Fleming S, Dirr E, Polinski NK, Trojanowski JQ, Lee VM, Sortwell CE, 2015. Intrastriatal injection of pre-formed mouse α-synuclein fibrils into rats triggers α-synuclein pathology and bilateral nigrostriatal degeneration. Neurobiol. Dis 82, 185–199. 10.1016/j.nbd.2015.06.003. [PubMed: 26093169]

Peter I, Dubinsky M, Bressman S, Park A, Lu C, Chen N, Wang A, 2018. Anti-tumor necrosis factor therapy and incidence of Parkinson disease among patients with inflammatory bowel disease. JAMA Neurol. 75, 939–946. 10.1001/jamaneurol.2018.0605. [PubMed: 29710331]

Polinski NK, Volpicelli-Daley LA, Sortwell CE, Luk KC, Cremades N, Gottler LM, Froula J, Duffy MF, Lee VMY, Martinez TN, Dave KD, 2018. Best practices for generating and using alpha-Synuclein pre-formed fibrils to model Parkinson's disease in rodents. J. Parkinsons Dis 8, 303–322. 10.3233/JPD-171248. [PubMed: 29400668]

Przanowski P, Dabrowski M, Ellert-Miklaszewska A, Kloss M, Mieczkowski J, Kaza B, Ronowicz A, Hu F, Piotrowski A, Kettenmann H, Komorowski J, Kaminska B, 2014. The signal transducers Stat1 and Stat3 and their novel target Jmjd3 drive the expression of inflammatory genes in microglia. J. Mol. Med 92, 239–254. 10.1007/s00109-013-1090-5. [PubMed: 24097101]

Qin XY, Zhang SP, Cao C, Loh YP, Cheng Y, 2016. Aberrations in peripheral inflammatory cytokine levels in Parkinson disease: a systematic review and meta-analysis. JAMA Neurol. 73, 1316–1324. 10.1001/jamaneurol.2016.2742. [PubMed: 27668667]

Reale M, Iarlori C, Thomas A, Gambi D, Perfetti B, Di Nicola M, Onofrj M, 2009. Peripheral cytokines profile in Parkinson's disease. Brain Behav. Immun 23, 55–63. 10.1016/j.bbi.2008.07.003. [PubMed: 18678243]

Sala Frigerio C, Wolfs L, Fattorelli N, Thrupp N, Voytyuk I, Schmidt I, Mancuso R, Chen W-T, Woodbury ME, Srivastava G, Möller T, Hudry E, Das S, Saido T, Karran E, Hyman B, Perry VH, Fiers M, de Strooper B, 2019. The major risk factors for Alzheimer's disease: age, sex, and genes modulate the microglia response to Aβ plaques. Cell Rep. 27, 1293–1306.e6. 10.1016/j.celrep.2019.03.099. [PubMed: 31018141]

Samii A, Etminan M, Wiens MO, Jafari S, 2009. NSAID use and the risk of Parkinson's disease. Drugs Aging 26, 769–779. 10.2165/11316780-000000000-00000. [PubMed: 19728750]

Sanchez-Guajardo V, Barnum CJ, Tansey MG, Romero-Ramos M, 2013. Neuroimmunological processes in Parkinson's disease and their relation to α-synuclein: microglia as the referee between neuronal processes and peripheral immunity. ASN Neuro 5, 113–139. 10.1042/AN20120066. [PubMed: 23506036]

Saunders A, Macosko EZ, Wysoker A, Goldman M, Krienen FM, de Rivera H, Bien E, Baum M, Bortolin L, Wang S, Goeva A, Nemesh J, Kamitaki N, Brumbaugh S, Kulp, McCarroll SA, 2018. Molecular diversity and specializations among the cells of the adult mouse brain. Cell. doi: 10.1016/j.cell.2018.07.028.

Scheiblich H, Bousset L, Schwartz S, Griep A, Latz E, Melki R, Heneka MT, 2021. Microglial NLRP3 Inflammasome activation upon TLR2 and TLR5 ligation by distinct α-Synuclein assemblies. J. Immunol 207, 2143–2154. 10.4049/jimmunol.2100035. [PubMed: 34507948]

Schröder B, 2016. The multifaceted roles of the invariant chain CD74 — more than just a chaperone. Biochim. Biophys. Acta (BBA) – Mol. Cell Res 1863, 1269–1281. 10.1016/j.bbamcr.2016.03.026.

Smajić S, Prada-Medina CA, Landoulsi Z, Ghelfi J, Delcambre S, Dietrich C, Jarazo J, Henck J, Balachandran S, Pachchek S, Morris CM, Antony P, Timmermann B, Sauer S, Pereira SL, Schwamborn JC, May P, Grünewald A, Spielmann M, 2022a. Single-cell sequencing of human midbrain reveals glial activation and a Parkinson-specific neuronal state. Brain 145, 964–978. 10.1093/brain/awab446. [PubMed: 34919646]

Smajić S, Prada-Medina CA, Landoulsi Z, Ghelfi J, Delcambre S, Dietrich C, Jarazo J, Henck J, Balachandran S, Pachchek S, Morris CM, Antony P, Timmermann B, Sauer S, Pereira SL, Schwamborn JC, May P, Grünewald A, Spielmann M, 2022b. Single-cell sequencing of human midbrain reveals glial activation and a Parkinson-specific neuronal state. Brain 145, 964–978. 10.1093/brain/awab446. [PubMed: 34919646]

Srinivasan K, Friedman BA, Larson JL, Lauffer BE, Goldstein LD, Appling LL, Borneo J, Poon C, Ho T, Cai F, Steiner P, van der Brug MP, Modrusan Z, Kaminker JS, Hansen DV, 2016. Untangling the brain's neuroinflammatory and neurodegenerative transcriptional responses. Nat. Commun 7, 11295. 10.1038/ncomms11295. [PubMed: 27097852]

Stefanova N, Fellner L, Reindl M, Masliah E, Poewe W, Wenning GK, 2011. Toll-like receptor 4 promotes α-synuclein clearance and survival of nigral dopaminergic neurons. Am. J. Pathol 179, 954–963. 10.1016/j.ajpath.2011.04.013. [PubMed: 21801874]

Stoll AC, Sortwell CE, 2022. Leveraging the preformed fibril model to distinguish between alpha-synuclein inclusion- and nigrostriatal degeneration-associated immunogenicity. Neurobiol. Dis 171, 105804 10.1016/j.nbd.2022.105804. [PubMed: 35764290]

Stoll AC, Kemp CJ, Patterson JR, Kubik M, Kuhn N, Benskey M, Duffy MF, Luk K, Sortwell CE, 2023. Microglial depletion does not impact alpha-synuclein aggregation or nigrostriatal degeneration in the rat preformed fibril model. Res. Sq 10.21203/rs.3.rs-2890683/v1.

Streit WJ, Xue QS, 2016. Microglia in dementia with Lewy bodies. Brain Behav. Immun 55, 191–201. 10.1016/j.bbi.2015.10.012. [PubMed: 26518296]

Sulzer D, Alcalay RN, Garretti F, Cote L, Kanter E, Agin-Liebes J, Liong C, McMurtrey C, Hildebrand WH, Mao X, Dawson VL, Dawson TM, Oseroff C, Pham J, Sidney J, Dillon MB, Carpenter C, Weiskopf D, Phillips E, Mallal S, Peters B, Frazier A, Lindestam Arlehamn CS, Sette A, 2017. T cells from patients with Parkinson's disease recognize α-synuclein peptides. Nature 546, 656–661. 10.1038/nature22815. [PubMed: 28636593]

Surendranathan A, Su L, Mak E, Passamonti L, Hong YT, Arnold R, Rodríguez PV, Bevan-Jones WR, Brain SAE, Fryer TD, Aigbirhio FI, Rowe JB, O'Brien JT, 2018. Early microglial activation and peripheral inflammation in dementia with Lewy bodies. Brain 141, 3415–3427. 10.1093/brain/awy265. [PubMed: 30403785]

Tansey MG, Romero-Ramos M, 2019. Immune system responses in Parkinson's disease: early and dynamic. Eur. J. Neurosci 49, 364–383. 10.1111/ejn.14290. [PubMed: 30474172]

Tansey MG, Wallings RL, Houser MC, Herrick MK, Keating CE, Joers V, 2022a. Inflammation and immune dysfunction in Parkinson disease. Nat. Rev. Immunol 10.1038/s41577-022-00684-6.

Tansey MG, Wallings RL, Houser MC, Herrick MK, Keating CE, Joers V, 2022b. Inflammation and immune dysfunction in Parkinson disease. Nat. Rev. Immunol 10.1038/s41577-022-00684-6.

Tarutani A, Suzuki G, Shimozawa A, Nonaka T, Akiyama H, Hisanaga S, Hasegawa M, 2016. The effect of fragmented pathogenic α-Synuclein seeds on prion-like propagation. J. Biol. Chem 291, 18675–18688. 10.1074/jbc.M116.734707. [PubMed: 27382062]

Terada T, Yokokura M, Yoshikawa E, Futatsubashi M, Kono S, Konishi T, Miyajima H, Hashizume T, Ouchi Y, 2016. Extrastriatal spreading of microglial activation in Parkinson's disease: a

positron emission tomography study. Ann. Nucl. Med 30, 579–587. 10.1007/s12149-016-1099-2. [PubMed: 27299437]

Utz SG, Greter M, 2019. Checking macrophages at the border. Nat. Neurosci 22, 848–850. 10.1038/s41593-019-0411-6. [PubMed: 31061495]

Volpicelli-Daley LA, Luk KC, Patel TP, Tanik SA, Riddle DM, Stieber A, Meaney DF, Trojanowski JQ, Lee VMY, 2011. Exogenous α-Synuclein fibrils induce Lewy body pathology leading to synaptic dysfunction and neuron death. Neuron 72, 57–71. 10.1016/j.neuron.2011.08.033. [PubMed: 21982369]

Volpicelli-Daley LA, Luk KC, Lee VMY, 2014. Addition of exogenous α-synuclein preformed fibrils to primary neuronal cultures to seed recruitment of endogenous α-synuclein to Lewy body and Lewy neurite-like aggregates. Nat. Protoc 9, 2135–2146. 10.1038/nprot.2014.143. [PubMed: 25122523]

Williams GP, Marmion DJ, Schonhoff AM, Jurkuvenaite A, Won WJ, Standaert DG, Kordower JH, Harms AS, 2020. T cell infiltration in both human multiple system atrophy and a novel mouse model of the disease. Acta Neuropathol. 139, 855–874. 10.1007/s00401-020-02126-w. [PubMed: 31993745]

Williams-Gray CH, Wijeyekoon R, Yarnall AJ, Lawson RA, Breen DP, Evans JR, Cummins GA, Duncan GW, Khoo TK, Burn DJ, Barker RA, 2016. Serum immune markers and disease progression in an incident Parkinson's disease cohort (ICICLE-PD). Mov. Disord 31, 995–1003. 10.1002/mds.26563. [PubMed: 26999434]

Yacoubian TA, Fang YHD, Gerstenecker A, Amara A, Stover N, Ruffrage L, Collette C, Kennedy R, Zhang Y, Hong H, Qin H, McConathy J, Benveniste EN, Standaert DG, 2023. Brain and systemic inflammation in De novo Parkinson's disease. Mov. Disord 38, 743–754. 10.1002/mds.29363. [PubMed: 36853618]

Yamada T, Mcgeer PL, Mcgeer EG, 1992. Lewy bodies in Parkinson's disease are recognized by antibodies to complement proteins. Acta Neuropathol 84 (1), 100–104. 10.1007/BF00427222. [PubMed: 1502878]

Yun SP, Kam TI, Panicker N, Kim Sangmin, Oh Y, Park JS, Kwon SH, Park YJ, Karuppagounder SS, Park H, Kim Sangjune, Oh N, Kim NA, Lee Saebom, Brahmachari S, Mao X, Lee JH, Kumar M, An D, Kang SU, Lee Y, Lee KC, Na DH, Kim D, Lee SH, Roschke VV, Liddelow SA, Mari Z, Barres BA, Dawson VL, Lee Seulki, Dawson TM, Ko HS, 2018. Block of A1 astrocyte conversion by microglia is neuroprotective in models of Parkinson's disease. Nat. Med 24, 931–938. 10.1038/s41591-018-0051-5. [PubMed: 29892066]

Zamanian JL, Xu L, Foo LC, Nouri N, Zhou L, Giffard RG, Barres BA, 2012. Genomic analysis of reactive astrogliosis. J. Neurosci 32, 6391–6410. 10.1523/JNEUROSCI.6221-11.2012. [PubMed: 22553043]

Zhang PF, Gao F, 2022. Neuroinflammation in Parkinson's disease: a meta-analysis of PET imaging studies. J. Neurol 10.1007/s00415-021-10877-z.

Zhao Y, Ma C, Chen C, Li S, Wang Y, Yang T, Stetler RA, Bennett MVL, Dixon CE, Chen J, Shi Y, 2022. STAT1 contributes to microglial/macrophage inflammation and neurological dysfunction in a mouse model of traumatic Brain injury. J. Neurosci 42, 7466–7481. 10.1523/JNEUROSCI.0682-22.2022. [PubMed: 35985835]

Zhong J, Tang G, Zhu J, Wu W, Li G, Lin X, Liang L, Chai C, Zeng Y, Wang F, Luo L, Li J, Chen F, Huang Z, Zhang X, Zhang Y, Liu H, Qiu X, Tang S, Chen D, 2021. Single-cell brain atlas of Parkinson's disease mouse model. J. Genet. Genomics 48, 277–288. 10.1016/j.jgg.2021.01.003. [PubMed: 34052184]

Zimmermann M, Brockmann K, 2022. Blood and cerebrospinal fluid biomarkers of inflammation in Parkinson's disease. J. Parkinsons Dis 10.3233/JPD-223277.

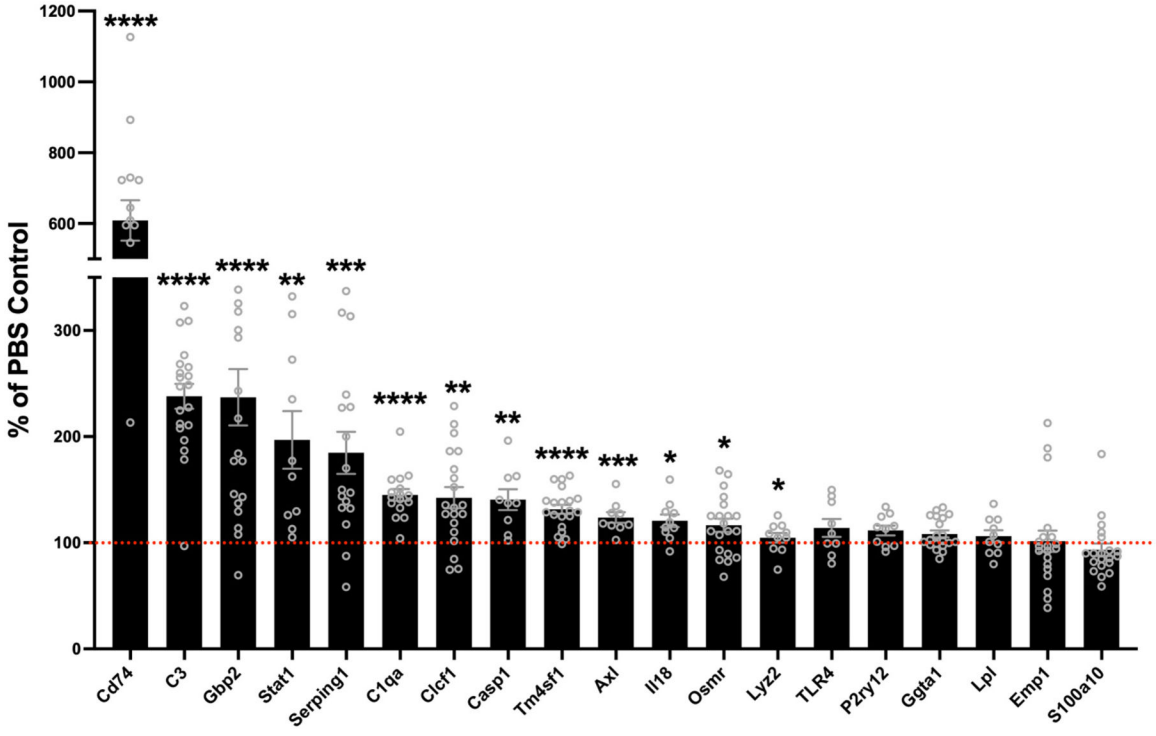

Fig. 1.

Synucleinopathy increases the expression of inflammatory associated transcripts in the SN. Rats received intrastriatal injection of alpha-synuclein preformed fibrils (α-syn PFFs) or phosphate buffered saline (PBS) control and were euthanized 2-months post-injection. Droplet digital PCR (ddPCR) was used to quantify immune transcripts in the ipsilateral substantia nigra (SN). Individual data points represent the gene of interest normalized to the reference gene, ribosomal protein L13 (*Rpl13)*, and expressed as percent of PBS control, while bars represent group means ± standard error of the mean (n = 10–20/group). Significant increases were observed in *Cd74*, *C3, Gbp*2, *Stat1, Serping1, C1qa, Clcf1, Casp1, Tm4sf1, Axl, IL18, Osmr*, *and Lyz2*. Genes not significantly altered in the SN of α-syn PFF treated animals compared to PBS controls include *Tlr4, P2ry12*, *Ggta1*, *Lpl*, *EMP1*, and *S100a10*. Three data points for *Gbp2* and 4 data points for *Cd74* are not visible on the graph due to the break in Y axis. *$p < 0.05$, **$p < 0.002$, ***$p < 0.0009$, ****p < 0.0001 utilizing the students t-test to compare gene expression in the ipsilateral SN of α-syn PFF versus PBS injected rats.

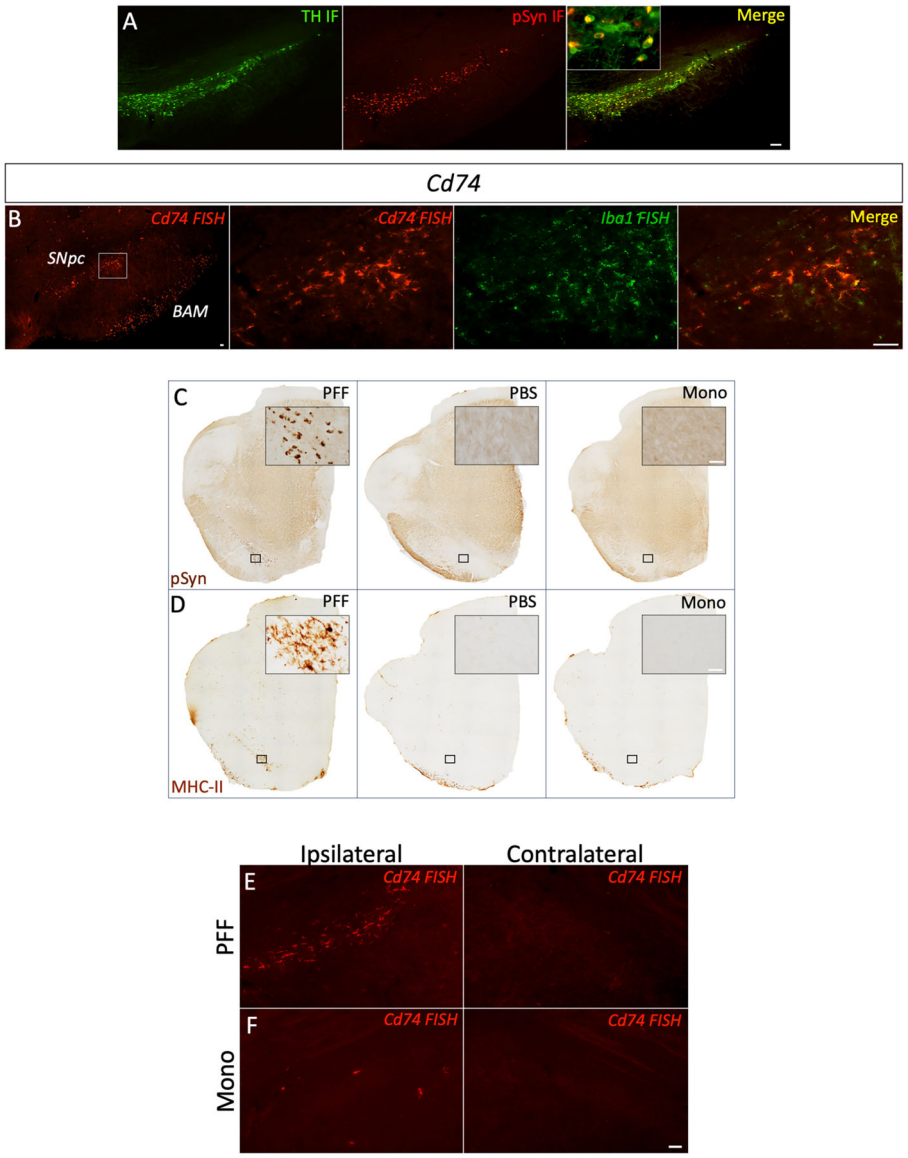

Fig. 2.

Intrastriatal injection of α-syn PFFs, but not PBS or α-syn monomer, leads to microglial *Cd74* expression in the ipsilateral SNpc. Rats received intrastriatal injections of alpha-synuclein preformed fibrils (α-syn PFFs), α-syn monomer or phosphate buffered saline (PBS) vehicle and were euthanized 2 months post-injection.

A. Representative immunofluorescence (IF) images of tyrosine hydroxylase (TH) neurons (green) containing serine 129 phosphorylated α-synuclein (pSyn) aggregates (red) in the SNpc ipsilateral to the α-syn PFF injected striatum. Inset in right panel shows high magnification image of pSyn+/TH+ neurons.

B. Fluorescent in situ hybridization (FISH) reveals *Cd74* (red) expression in border associated macrophages (BAM) and in *Iba1* mRNA positive (Green) microglia in the ipsilateral SNpc following PFF injection.

C: Representative images of pSyn immunoreactive neurons in the SNpc following PFF injection (left panel) but not PBS (middle panel) or α-syn monomer injection (right panel). Insets in (C) show high magnification images of the area in box in corresponding low magnification images.

D: Representative images of major histocompatibility complex class II (MHC-II) immunoreactive microglia in the SNpc following PFF injection (left panel) but not PBS (middle panel) or α-syn monomer injection (right panel). Insets in (D) show high magnification images of the area in box in corresponding low magnification images.

E. *Cd74* expression is observed in the ipsilateral SNpc following α-syn PFF injection (left panel) but not in the contralateral SNpc (right panel).

F. *Cd74* expression is minimal in the ipsilateral SNpc following α-syn monomer injection (left panel) and completely absent in the contralateral SNpc. Scale bars in A = 100 μm, B–F = 50 μm.

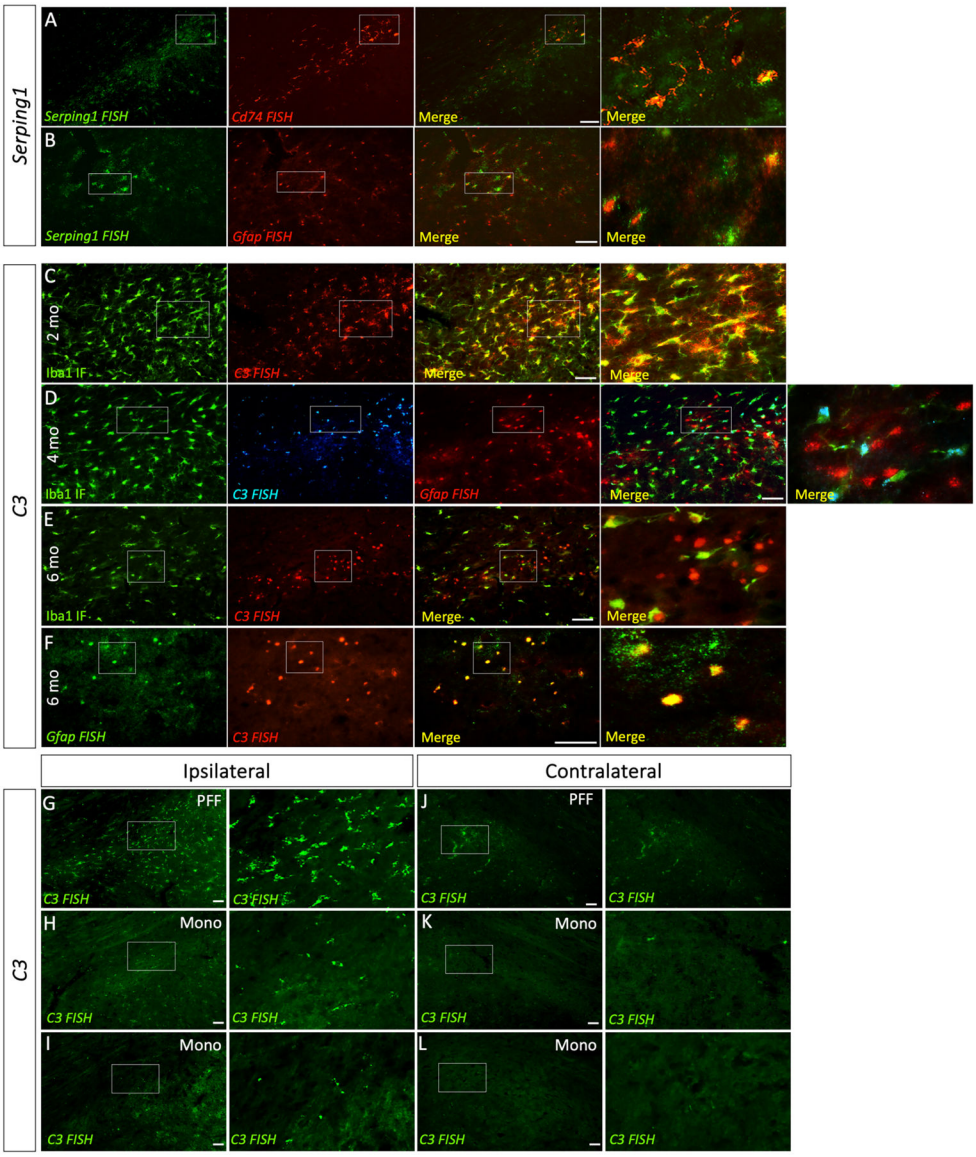

Fig. 3.

Cellular localization of *Serping1 and C3* mRNA in the SNpc of PFF Injected Rats.

Rats received intrastriatal injections of alpha-synuclein preformed fibrils (α-syn PFFs) or α-syn monomer and were euthanized 2, 4 or 6 months post-injection. Fluorescent in situ hybridization (FISH) was used to detect *Serping1 or C3* mRNA in either glial fibrillary acidic protein mRNA positive (*Gfap*+) astrocytes or microglia labeled for Ionized calcium-binding adaptor molecule-1 (Iba1) or *Cd74* in the substantia nigra pars compacta (SNpc). (A–B) Show *Serping1* expression localizes to both astrocytes and microglia in the SNpc 2 months following PFF injection.

A: Representative images showing *Serping1* FISH (green) colocalizing with *Cd74* FISH (red) in the ipsilateral SNpc, 2 months post α-syn PFF injection.

B: Representative images showing *Serping1* FISH (green) colocalizing with *Gfap* FISH (red) in the ipsilateral SNpc, 2 months post α-syn PFF injection. (C–F) Show *C3* expression in the SNpc shifting from microglia to astrocytes over time following α-syn PFF injection.
C: Representative images showing complete colocalization of *C3* FISH (red) with Iba1 IF (green) positive microglia in the ipsilateral SNpc, 2 months post α-syn PFF injection.
D: Representative images showing complete colocalization of *C3* FISH (cyan) with Iba1 IF (green) and lack of colocalization with *Gfap* FISH (red) in the ipsilateral SNpc 4 months post α-syn PFF injection.
E. Representative images showing minimal colocalization of *C3* FISH (red) with Iba1 IF (green) in the ipsilateral SNpc 6 months post α-syn PFF injection.
F: Representative images showing colocalization of *C3* FISH (red) with *Gfap* FISH (green) in the ipsilateral SNpc 6 months post α-syn PFF injection. (G–L) Show *C3* expression is abundantly upregulated in the ipsilateral SNpc of α-syn PFF injected rats with minimal upregulation in the ipsilateral SNpc α-syn monomer injected rats, 2 months post-injection.
G: Representative images of *C3* FISH in the ipsilateral SNpc of α-syn PFF injected rats with minimal *C*3 FISH signal in the contralateral SNpc (**J**), 2 months post-injection.
H–I: Representative images of *C3* FISH in the ipsilateral SNpc of α-syn monomer injected rats with minimal upregulation in the contralateral SNpc (**K–L**), 2 months post-injection. High magnification images in all panels represent the area in the box in the corresponding low magnification images to the left. Scale bars in low magnification panels is 50 μm and applies to all low magnification panels.

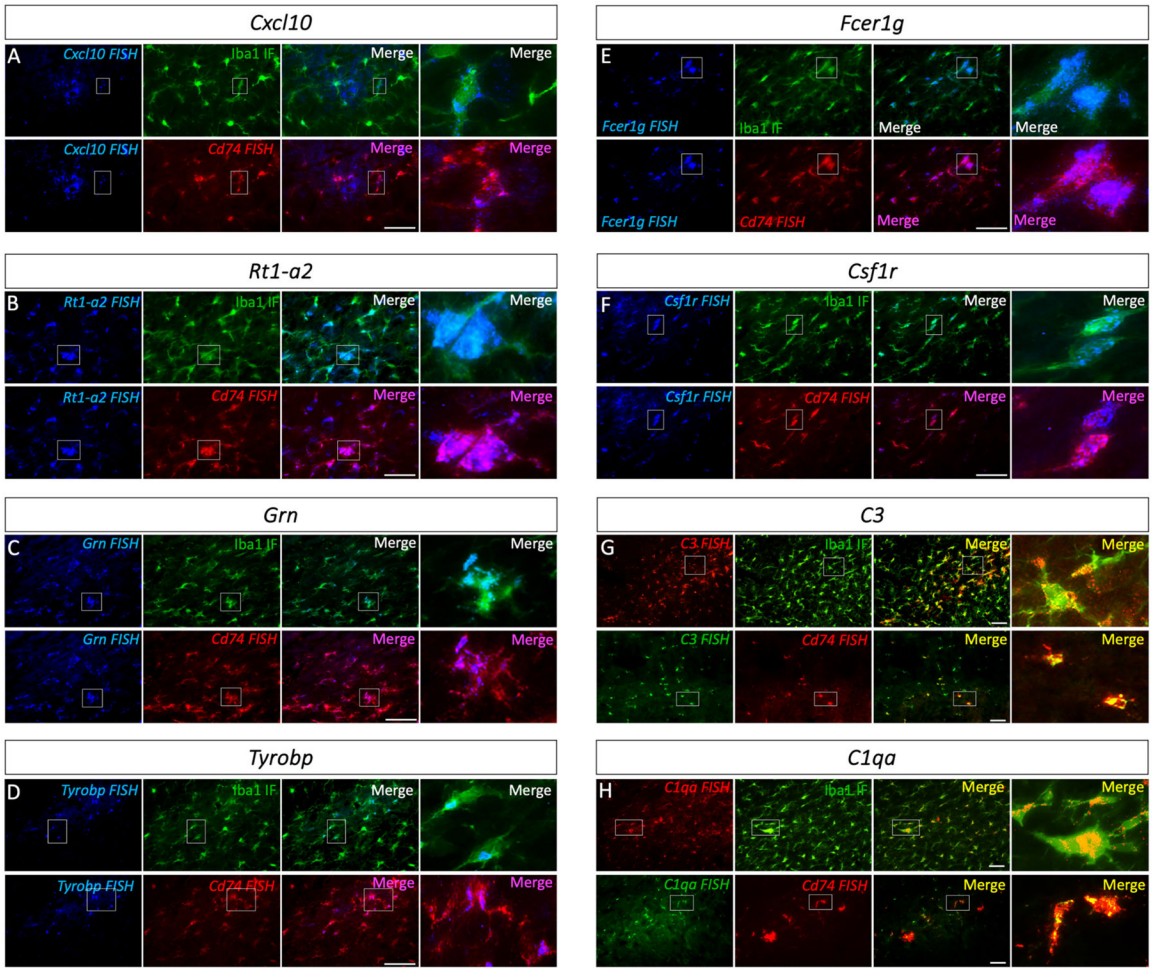

Fig. 4.

Cd74+ microglia upregulate innate immune transcripts in the SNpc of α-syn PFF injected rats. Rats received intrastriatal injection of alpha-synuclein pre-formed fibrils (α-syn PFFs). Two months post-injection fluorescent in situ hybridization (FISH) combined with immunofluorescence (IF) was performed in the ipsilateral substantia nigra pars compacta (SNpc) to localize innate immune transcripts to either ionized calcium adaptor binding molecule-1 (Iba1) immunoflourescent (IF) microglia or *Cd74* mRNA positive microglia. All transcripts analyzed (*CxCl10*, *Rt1-a2*, *Grn*, *Tyrobp*, *Fcer1g*, *Csf1r*, *C3*, *C1qa)* colocalized with Iba1 and *Cd74*, indicative of microglial expression.

A: Representative images of *Cxcl10* FISH (Blue), Iba1 IF (Green), and *Cd74* FISH (Red).

B: Representative images of *Rt1-a2* FISH (Blue), Iba1 IF (Green), and *Cd74* FISH (Red).

C: Representative images of *Grn* FISH (Blue), Iba1 IF (Green), and *Cd74* FISH (Red).

D: Representative images of *Tyrobp* FISH (Blue), Iba1 IF (Green), and *Cd74* FISH (Red).

E: Representative images of *Fcer1g* FISH (Blue), Iba1 IF (Green), and *Cd74* FISH (Red).

F: Representative images of *Csf1r* FISH (Blue), Iba1 IF (Green), and *Cd74* FISH (Red).

G: Representative images of *C3* FISH (Red top panel, Green lower panel), Iba1 IF (Green) and *Cd74* mRNA (Red).

H: Representative images of *C1qa* FISH (Red top panel, Green lower panel), Iba1 IF (Green) and *Cd74* mRNA (Red).

High magnification images in all panels represent the area in the box in the corresponding low magnification panels to the left. Scale bar in low magnification panels is 50um and applies to all low magnification panels. All images taken in the ipsilateral SNpc.

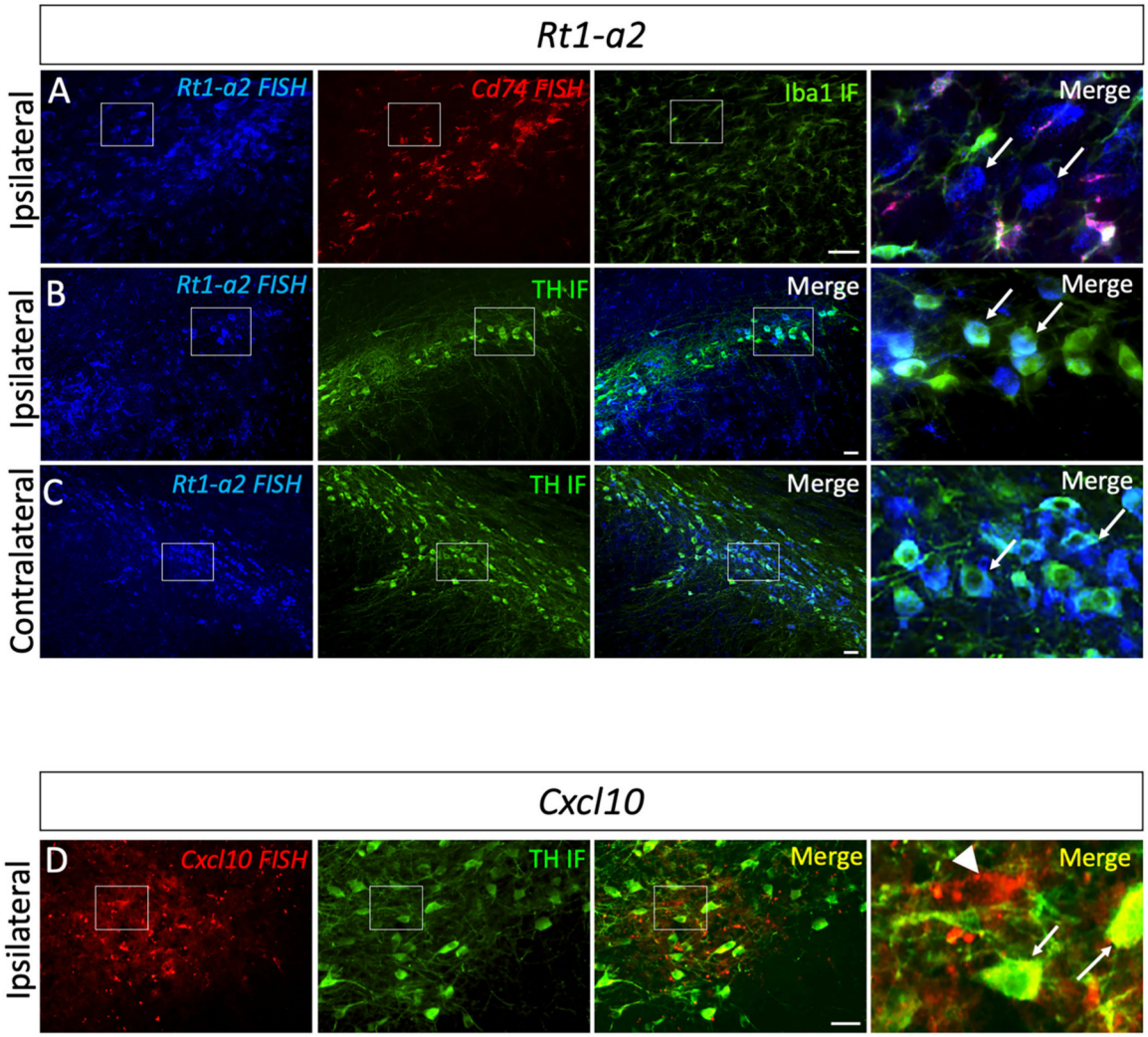

Fig. 5.

Expression of *Rt1-a2* and *Cxcl10* by dopamine neurons in the SNpc. Rats received intrastriatal injection of alpha-synuclein preformed fibrils (α-syn PFFs). Two months post-injection fluorescent in situ hybridization (FISH) combined with immunofluorescence (IF) was performed in the ipsilateral (A–B, D) or contralateral (C) substantia nigra pars compacta (SNpc) to analyze expression of *Rt1-a2* and *Cxcl10* in tyrosine hydroxylase positive (TH+) neurons or ionized calcium adaptor binding molecule-1 positive (Iba1+)/*Cd74*+ microglia.

A: Representative images of *Rt1-a2* FISH (Blue), *Cd74* FISH (Red) and Iba1 IF (Green) in the ipsilateral SNpc. Arrows in right panel indicate examples of *Rt1-a2*+ cells that are *Cd74*−/Iba1−.

B: Representative images of *Rt1-a2* FISH *(Blue)* and TH IF (Green) in the ipsilateral SNpc. Arrows in the right panel indicate examples of colocalization of *Rt1-a2* FISH with TH IF.

C: Representative images of *Rt1-a2* FISH (blue) and TH IF (Green) in the contralateral SNpc. Arrows in the right panel indicate examples of colocalization of *Rt1-a2* FISH with TH IF.

D. Representative images of *Cxcl10* FISH (red) and TH IF (Green) in the ipsilateral SNpc. Arrows in the right panel indicate examples of colocalization of *Cxcl10* FISH with TH IF, arrowhead indicates example of *Cxcl10* FISH signal that morphologically resembles a nigral neuron soma but does not colocalize with TH IF (presumably a TH-neuron). High magnification images in all panels represent the area in the box in the corresponding low magnification panels to the left. Scale bars in low magnification panels is 50 μm and applies to all low magnification panels.

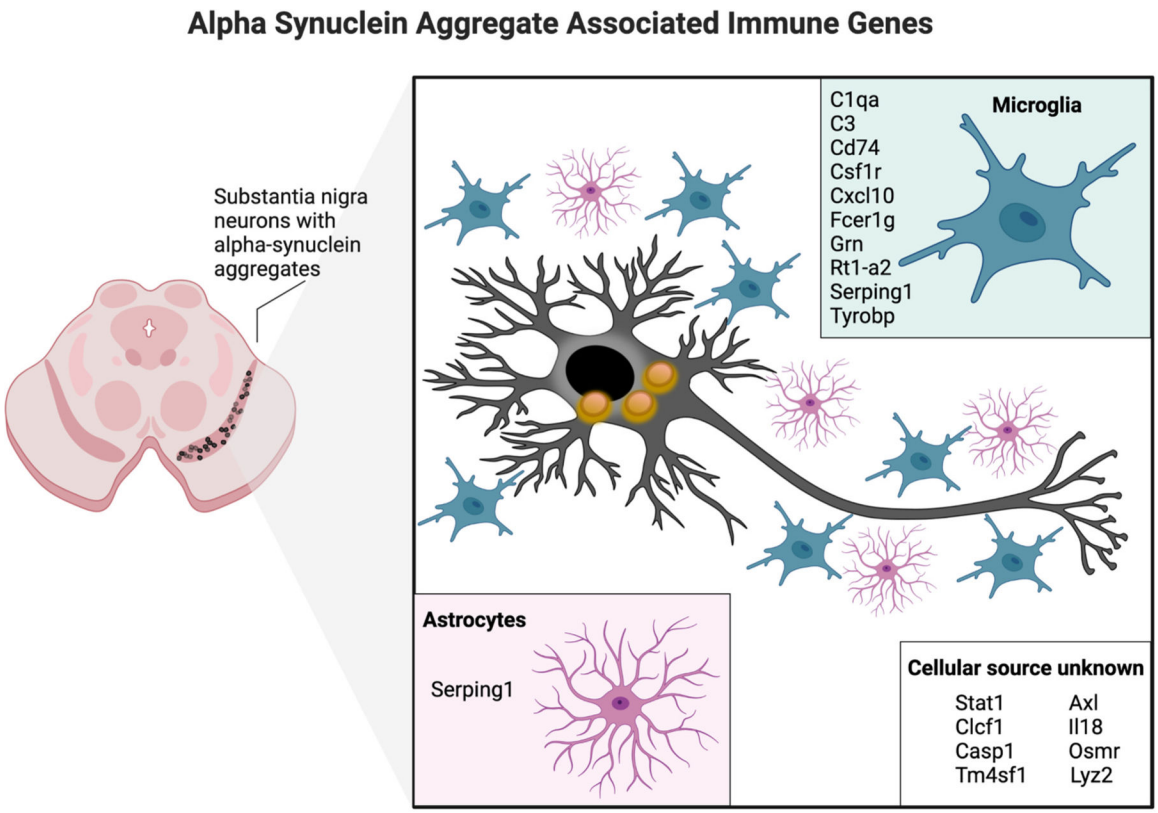

Fig. 6.

Glial localization of α-syn aggregate associated immune genes. Glial cells in the immediate proximity of alpha synuclein (α-syn) aggregate containing neurons in substantia nigra pars compacta (SNpc) upregulate specific immune genes 2-months following intrastriatal injection α-syn pre-formed fibrils (PFFs). Upregulated genes include *Serping1* in astrocytes, and *Cxcl10, Rt1-a2, Grn, Csf1r, C3, C1qa, Tyrobp, Serping1* and *Fcer1g* in *Cd74*+ microglia. This α-syn aggregate associated microglial phenotype implicates the involvement of multiple immune pathways in the SNpc microglial response to α-syn aggregation. Importantly, these immune genes are upregulated in SNpc microglia prior to degeneration, suggesting they may participate in a neurotoxic inflammatory response to synucleinopathy. Interestingly, during the degeneration phase (6 months post PFF) upregulation of C3 is no longer observed in microglia but instead localized to astrocytes. Using our ddPCR approach we identified additional neuroinflammatory genes, including *Gbp*2, *Stat1, Clcf1, Casp1, Tm4sf1, Axl, IL18, Osmr, and Lyz2*, all of which are significantly upregulated in inclusion bearing nigral SN tissue compared to PBS controls, although the cellular source of these genes is currently unknown. Findings in the present study suggest that deposition of pathological α-syn in the SNpc increases immune functions related to phagocytosis, microglial regulation, astrocyte activation, lysosomal function, cell proliferation, complement cascade, cytokine signaling, and B cell activation. Created with BioRender.com